AD NUMBER

ADB004733

LIMITATION CHANGES

TO:

Approved for public release; distribution is unlimited.

FROM:

Distribution authorized to U.S. Gov't. agencies only; Administrative/Operational Use; MAR 1975. Other requests shall be referred to Federal Aviation Administration, Supersonic Transport Office, 800 Independence Avenue, SW, Washington, DC 20590. This document contains export-controlled technical data.

AUTHORITY

faa ltr, 26 apr 1977

Report No. FAA-SS-73-11-6

SST Technology Follow-On Program—Phase II NOISE SUPPRESSOR/NOZZLE DEVELOPMENT VOLUME VI

PERFORMANCE TECHNOLOGY—THRUST AND FLOW CHARACTERISTICS OF A REFERENCE MULTITUBE NOZZLE WITH EJECTOR

F. Pearlman R. Armstrong

Boeing Commercial Airplane Company
P.O. Box 3707
Seattle, Washington 98124

D6-43302

March 1975

FINAL REPORT

Task III

Prepared for
FEDERAL AVIATION ADMINISTRATION
Supersonic Transport Office
800 Independence Avenue, S.W.
Washington, D.C. 20590

The contents of this report reflect the views of the Boeing Commercial Airplane Company, which is responsible for the facts and the accuracy of the data presented herein. The contents do not necessarily reflect the official views or policy of the Department of Transportation. This report does not constitute a standard, specification, or regulation.

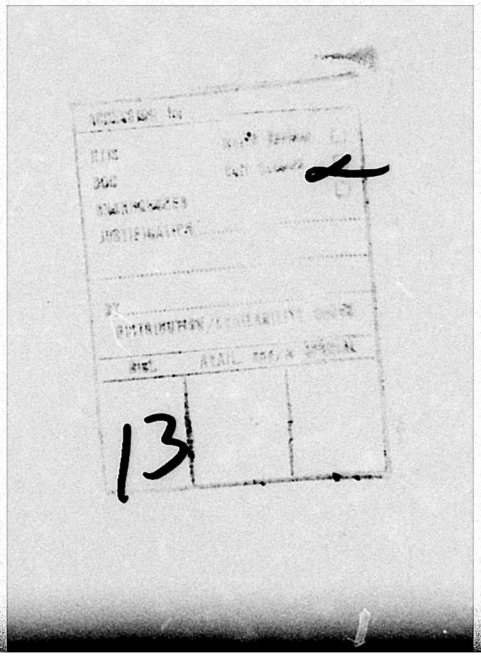

TECHNICAL REPORT STANDARD TITLE PAGE

1. Report No.	2. Government Accession No.	3. Recipient's Catalog No.
FAA-SS73-11-6		

4. Title and Subtitle

SST TECHNOLOGY FOLLOW-ON PROGRAM—PHASE II.
Noise Suppressor/Nozzle Development. Volume VI.
Performance Technology—Thrust and Flow Characteristics
of a Reference Multitube Nozzle With Ejector.

5. Report Date: Mar[illegible]975

6. Performing Organization Code:

7. Author(s)

F. Pearlman R. S. Armstrong

8. Performing Organization Report No.: D6-43302

9. Performing Organization Name and Address

Boeing Commercial Airplane Company
P.O. Box 3707
Seattle, Washington 98124

10. Work Unit No.:

11. Contract or Grant No.: DOT-FA-72WA-2893

12. Sponsoring Agency Name and Address

Federal Aviation Administration
Supersonic Transport Office
800 Independence Avenue, S.W.
Washington, D.C. 20590

13. Type of Report and Period Covered: Final Report, Task III,

14. Sponsoring Agency Code:

15. Supplementary Notes

Distribution limited to U.S. Govt. agencies only! Other requests for this document must be referred to

16. Abstract

Static tests are conducted to establish reference performance levels for a round convergent nozzle and a 3.3 area ratio, 37-tube suppressor nozzle. After assessing bare nozzle performance characteristics, ejector shrouds are added, and the effect of secondary inlet changes and ejector length change on thrust is established. Pressure measurements on nozzle/ejector surfaces are correlated with measured thrust. The secondary flow is measured, and the flow conditions inside the ejectors are established by performing pressure/temperature traverses.

17. Key Words	18. Distribution Statement
Suppressor nozzle, Nozzle performance Multitube suppressor ejector, SST, Ejector performance, Ejector air handling	

19. Security Classif. (of this report)	20. Security Classif. (of this page)	21. No. of Pages	22. Price
Unclassified	Unclassified		

Form DOT F 1700.7 (8-69)

390 145 ✓

PREFACE

This is one of a series of final reports on noise and propulsion technology submitted by the Boeing Commercial Airplane Company, Seattle, Washington, 98124, in fulfillment of Task III of Department of Transportation Contract DOT-FA-72WA-2893, dated 1 February 1972.

To benefit utilization of technical data developed by the noise suppressor and nozzle development program, the final report is divided into 10 volumes covering key technology areas and a summary of total program results. The 10 volumes are issued under the master title, "Noise Suppressor/Nozzle Development." Detailed volume breakdown is as follows:

			Report No.
Volume I	–	Program Summary	FAA-SS-73-11-1
Volume II	–	Noise Technology	FAA-SS-73-11-2
Volume III	–	Noise Technology–Backup Data Report	FAA-SS-73-11-3
Volume IV	–	Performance Technology Summary	FAA-SS-73-11-4
Volume V	–	Performance Technology–The Effect of Initial Jet Conditions on a 2-D Constant Area Ejector	FAA-SS-73-11-5
Volume VI	–	Performance Technology–Thrust and Flow Characteristics of a Reference Multitube Nozzle With Ejector	FAA-SS-73-11-6
Volume VII	–	Performance Technology–A Guide to Multitube Suppressor Nozzle Static Performance: Trends and Trades	FAA-SS-73-11-7
Volume VIII	–	Performance Technology–Multitube Suppressor/Ejector Interaction Effects on Static Performance (Ambient and 1150° F Jet Temperature)	FAA-SS-73-11-8
Volume IX	–	Performance Technology–Analysis of the Low-Speed Performance of Multitube Suppressor/Ejector Nozzles (0-167 kn)	FAA-SS-73-11-9
Volume X	–	Advanced Suppressor Concepts and Full-Scale Tests	FAA-SS-73-11-10

This report is volume VI of the series and was prepared by the Propulsion Research Staff of the Boeing Commercial Airplane Company.

SUMMARY

A round convergent reference nozzle and a 3.3 area ratio 37-tube, close packed array, suppressor nozzle are tested bare and with various ejector configurations in order to determine the relative differences in performance between configurations. The two reference nozzles tested at the hot nozzle test facility share the following design characteristics: they have the same primary flow area, the same exit plane station, and nacelles of identical outside diameter. The basic hardware differences between the round convergent nozzle and the multitube suppressor can be reflected as a difference in wetted areas, i.e., primary jet configuration, ramp areas, and base areas. These affect the baseline nozzle characteristics, which result in a lower discharge coefficient and a lower gross thrust coefficient for the multitube nozzle caused by increased internal skin friction and external drag. Both nozzles are tested with 3.7 area ratio cylindrical ejectors having similar inlets—either bellmouth or flight lip—and corresponding mixing lengths selected to allow for full mixing. The discharge coefficients remain identical to the baseline C_D. The gross thrust coefficients increase by similar amounts for both nozzle configurations. This increase, which is somewhat larger for a bellmouth inlet than for a flight lip, is caused by the change in the body forces near the ejector inlet and is governed by the variations of the lip suction.

Variations in ejector length closely affect the state of mixing at the end of the ejector; if the ejector is short, the flow is not fully mixed and performance drops drastically, as for the L/D = 1 ejector tested with the round convergent nozzle.

When the primary flow is heated to 1150° F, the bare nozzle performance is only modified by a very small percentage, but the nozzle ejector performance is decreased by a large amount for all the configurations studied. The body forces, mainly the lip suction, are decreased, leading to lower performance. The drop in performance is of the same magnitude for all fully mixed configurations and slightly less when the flow is partially mixed.

TABLE OF CONTENTS

LIST OF FIGURES

LIST OF TABLES

SYMBOLS AND ABBREVIATIONS

C_D	discharge coefficient corrected for temperature effects
C_{FG}	gross thrust coefficient
$C_{V_{int}}$	internal velocity coefficient
C_{WS}	secondary mass flow coefficient
D_B	base drag coefficient
F_{ID}	ideal primary thrust
L/D	ejector length to diameter ratio
P	pressure
P_E	ejector interior wall static pressure
PSNE	R/C nozzle external surface static pressure
PR	pressure ratio
P_{T_P}	primary flow total pressure
P_{AMB}	ambient pressure
psia	pounds per square inch absolute
q	dynamic pressure ($1/2\rho V^2$)
Re	Reynolds number
R/C	round convergent nozzle
R/37	37-tube reference suppressor nozzle
r	exit radius
T_{T_P}	primary flow total pressure
T_S	secondary total temperature
T_P	primary total temperature
W_S	secondary weight flow

W_P	primary weight flow
ΔP_T	total pressure loss
θ	momentum thickness

1.0 INTRODUCTION

During the DOT Phase I program (ref. 1) and NASA Lewis lined ejector test (ref. 2), a round convergent reference (R/C) nozzle was used to demonstrate the relative changes in performance and noise suppression properties between different configurations. Multitube nozzles have therefore been usually appraised in comparison with a nozzle of completely different noise characteristics.

The main purpose of the current reference nozzle test is to provide additional reference values of noise/performance characteristics that are similar to those of the suppressors being evaluated throughout the DOT/SST Phase II program. A 37-tube nozzle, R/37, was designed and periodically tested, along with the conventional R/C nozzle, to establish this additional reference performance.

This report is focused on the compared performance characteristics of the multitube and round convergent reference nozzles. It includes a detailed description of the hardware and instrumentation, a discussion of the baseline performance, ejector performance, and pumping characteristics, and a study of the downstream profiles.

2.0 TEST PROGRAM DESCRIPTION

2.1 TEST FACILITY

The reference nozzles were tested on the hot nozzle test facility located at North Boeing Field, Seattle, Washington. The facility is a single-axis thrust rig with an air supply capable of supplying up to 45 lb/sec. An in-line kerosene-type burner is mounted on the rig to supply hot flow. Temperature profiles at the test nozzle charging station were initially measured to ensure that they were within acceptable tolerances. (The variations being ±30° F from average.)

The primary flow rate was measured using a sonic venturi flow meter. The thrust was obtained with a load cell providing 0.25% of full-scale accuracy over a 1000-lb range. A 6-inch primary charging station instrumentation assembly, described in the instrumentation section, was used for area weighted total pressure and temperature measurements upstream of the nozzle.

2.2 RANGE OF VARIABLES

Static thrust, airflow, and jet flow characteristics are measured for two reference nozzles with various ejector configurations over a range of nozzle pressure ratios from 2 to 4 and ambient and 1150° F jet temperatures. A round convergent nozzle is tested with ejectors of area ratio 3.7 (where the ejector area ratio is defined as ejector flow area divided by nozzle exit area) and ejector length to diameter ratios of 3 and 6. A short ejector with length/diameter of one is tested with a 37-tube suppressor reference nozzle. Each ejector was tested with bellmouth and flight-type inlets.

2.3 TEST HARDWARE

- Round covergent, R/C, reference nozzle
  The R/C nozzle is a round, 10° convergent nozzle with a geometric flow area of 13.6 in^2 and a 12° boattail matched to the nacelle by a 40-in. radius curve segment.

- 37-tube reference suppressor nozzle
  The 37-tube suppressor has a 13.6 in^2 geometric flow area—similar to the R/C nozzle and mates to a 10-in. outside diameter nacelle. The number of tubes was selected as a representative value for good noise suppression based on previous testing. A 3.3 area ratio array of nearly uniform spaced tubes (where the nozzle area ratio is defined as the ratio of the base area to the periphery of the tubes over the geometric flow area) was chosen as a reference configuration to provide noise characteristics comparable with previous experience—such as the NASA Lewis lined ejector test, reference 2. In order to minimize nozzle boattail separation, a gradually sloping base was designed using a 40-in. boattail radius (radius/nacelle diameter = 4) tangent to the nacelle and terminating in a central hole. All tube exits were coplanar, and in order to maximize internal performance, convergent tube ends were selected. The two reference nozzles are illustrated in figure 1.

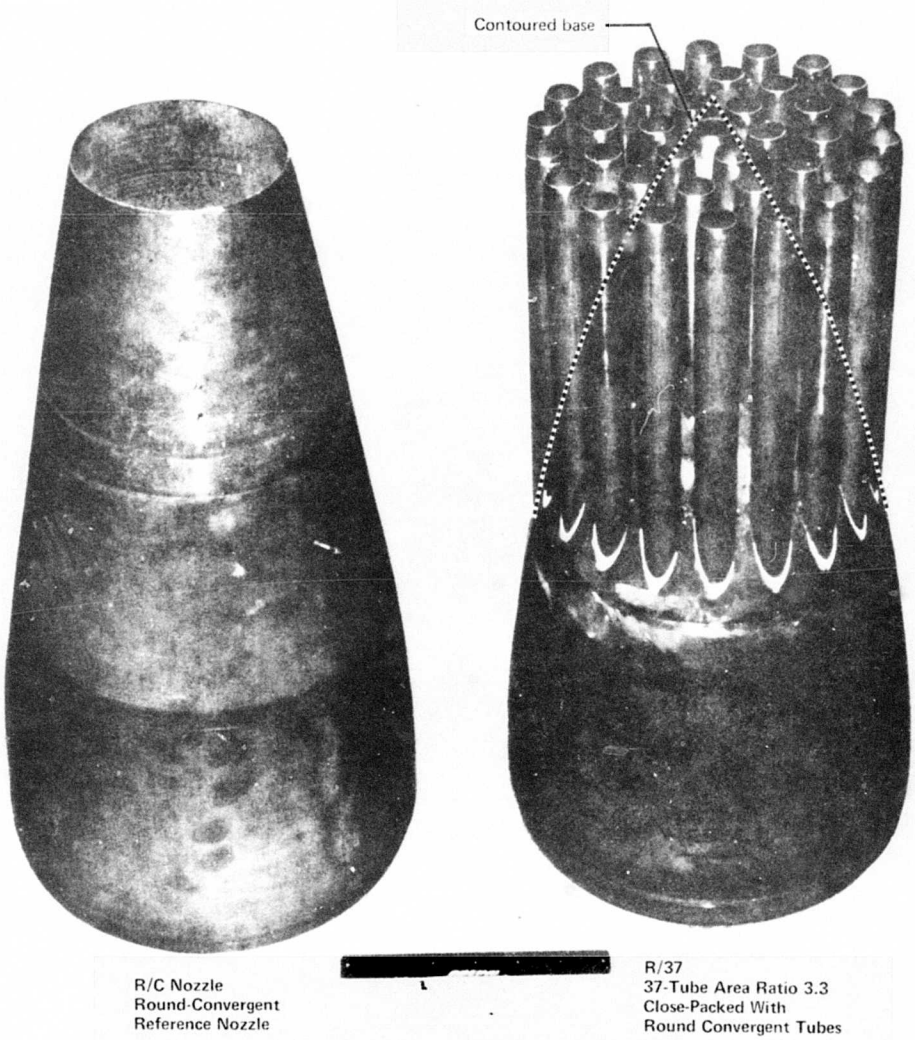

Figure 1.—R/C and R/37 Nozzles

The nozzle being tested was mounted directly on the 6-in. diameter instrumentation section during early portions of the program. Subsequently, a 4° half-angle diffuser was added between the instrumentation section and a short convergent section to which the test nozzle was mounted.

- Ejector configurations

  Two area ratio 3.7 cylindrical ejectors were used with the R/C nozzle. One ejector with a length to internal diameter ratio of 6 is designed to provide for a fully mixed flow (see ref. 3). The data are therefore comparable with analytical information obtained for one-dimensional mixing.

  The second ejector with a length-to-diameter ratio of 3 is expected to represent a partial mixing case. A comparison can therefore be made on the effect of mixing length of the ejectors. The R/37 uses a short ejector, L/D = 1, with a length to internal diameter ratio of 1 and a length to individual jet diameter ratio of 12 (see fig. 2). This provides the same ejector length to individual jet diameter ratio as the L/D = 6 ejector used with the R/C nozzle. Both of these configurations should allow fully mixed flow at the ejector exit.

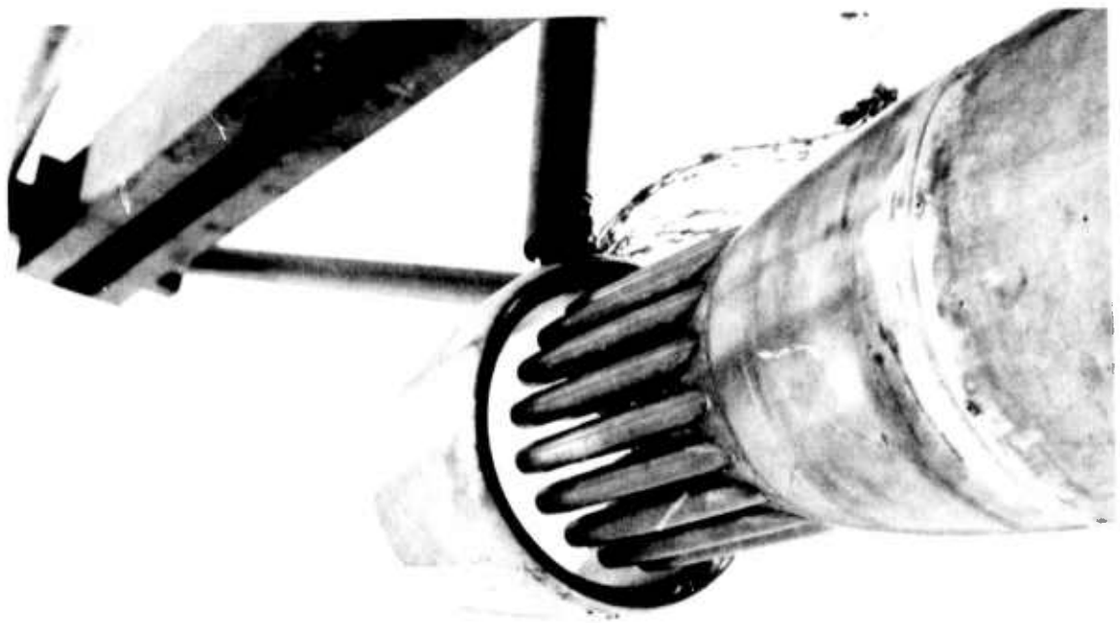

Figure 2.—R/37 Nozzle With 8 In. Ejector (L/D = 1) and Flight Lip Inlet

The R/C and R/37 share the following characteristics:

- 13.6-in^2 primary flow area
- 10-in. outside diameter nacelle
- Exit planes are at the same station
- 3.7 area ratio ejectors of corresponding mixing length (L/D = 6 for R/C and L/D = 1 for R/37) can be fitted with identical inlet lips

Two inlet lips are available for these ejectors—an elliptical flight lip and a bellmouth inlet fitted to the shroud to obtain the same secondary inlet area as the flight lip. The bellmouth is either rounded and terminated (see fig. 3) or extended by a cylindrical duct and a larger bellmouth. The latter provides for a section of annular secondary parallel flow upstream of the throat that is instrumented for secondary flow rate measurements. The round convergent nozzle with the L/D = 6 ejector and the large bellmouth is shown on figure 4 as installed on the test facility.

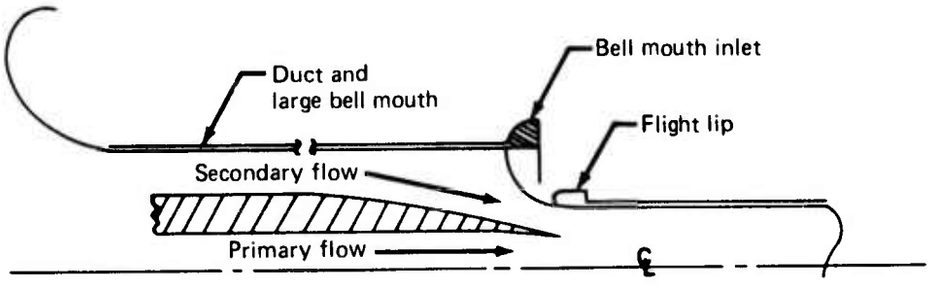

Figure 3.—Ejector Inlet Configuration

2.4 INSTRUMENTATION

In order to obtain accurate information on the primary flow upstream of the nozzle, a total pressure and temperature rake was designed for the 6 in. instrumentation section just upstream of the primary nozzle. The cruciform rake includes 14 area weighted total pressure probes distributed along the vertical axis and 14 area weighted total temperature shielded probes located along the horizontal axis. All these probes monitor values at the same axial station and provide for total temperature and pressure profiles at that station (primary nozzle charging station). When the large bellmouth is fitted to an ejector, it provides an annular secondary flow measuring station instrumented with a total temperature and pressure rake

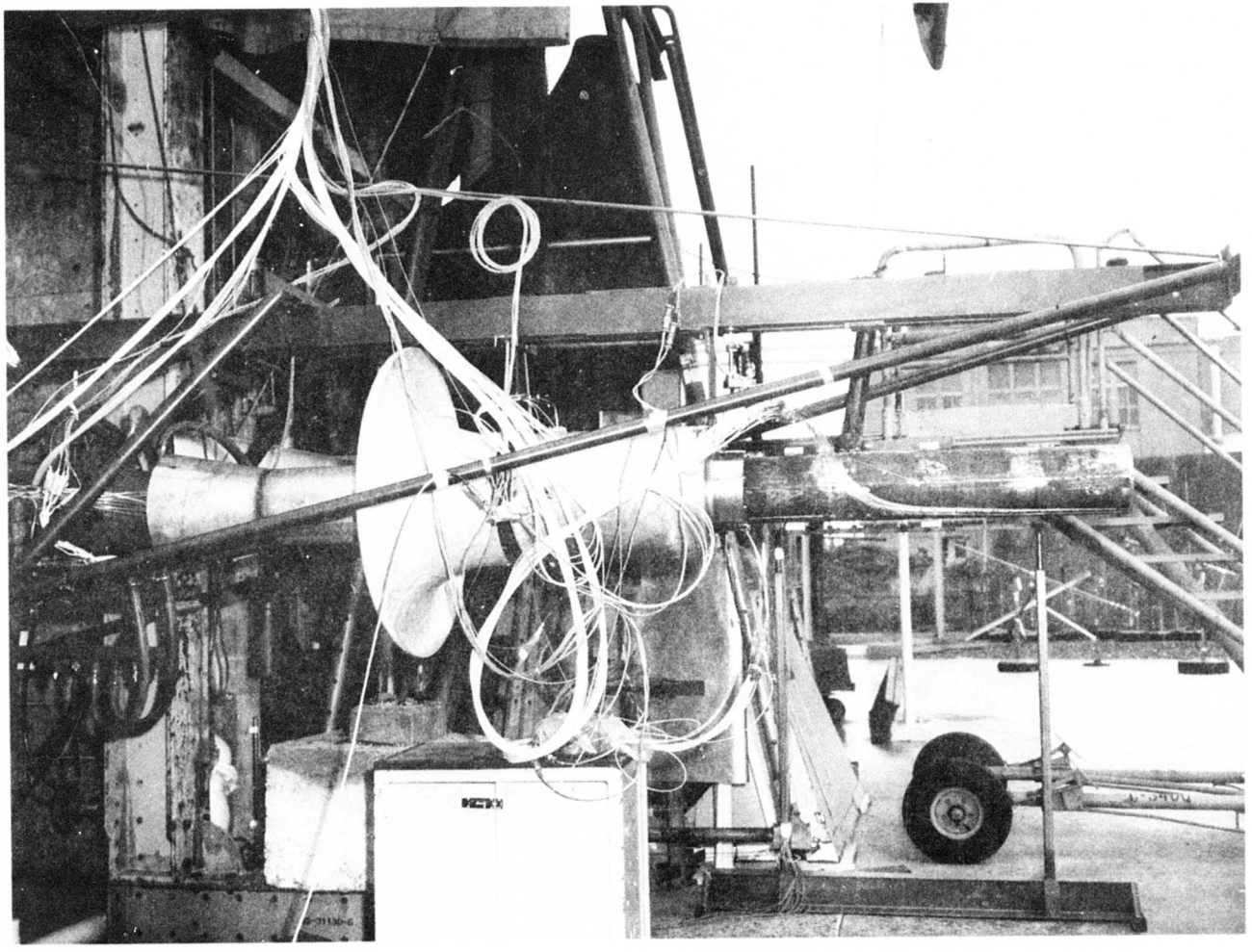

Figure 4.—Measurement of Secondary Mass Flow on Hot Nozzle Facility: R/C Nozzle With 48 In. Ejector (L/D = 6)

(see fig. 5). The latter consists of six area weighted total temperature probes placed horizontally across the flow and eight area weighted total pressure probes, divided into two rakes of four probes each, placed at the top and bottom of the annulus. This information is used in the calculation of the secondary flow rate.

Static pressure taps were located along the ramp of the R/C nozzle and along the base and ramp of the R/37 nozzle in order to obtain drag values. Three taps were located at the end of the tubes, providing for a local static pressure of the primary flow at the tube exits. The ramps of the R/37 and R/C nozzles were instrumented as indicated in figures 6 and 7. The ramp static pressures were used to calculate a ramp drag. Internal ejector static pressures were measured for the three ejectors to obtain information on the Mach number and the character of the flow, i.e., state of mixing within the ejector. (See figs. 8 and 9.)

A traversing mechanism containing total pressure and temperature probes was used to obtain jet flow profiles. This device can be either inserted into each ejector at stations of 0 (nozzle exit), 1, 3, and 6 ejector diameters, or it can be used as a freestanding unit downstream of the exit.

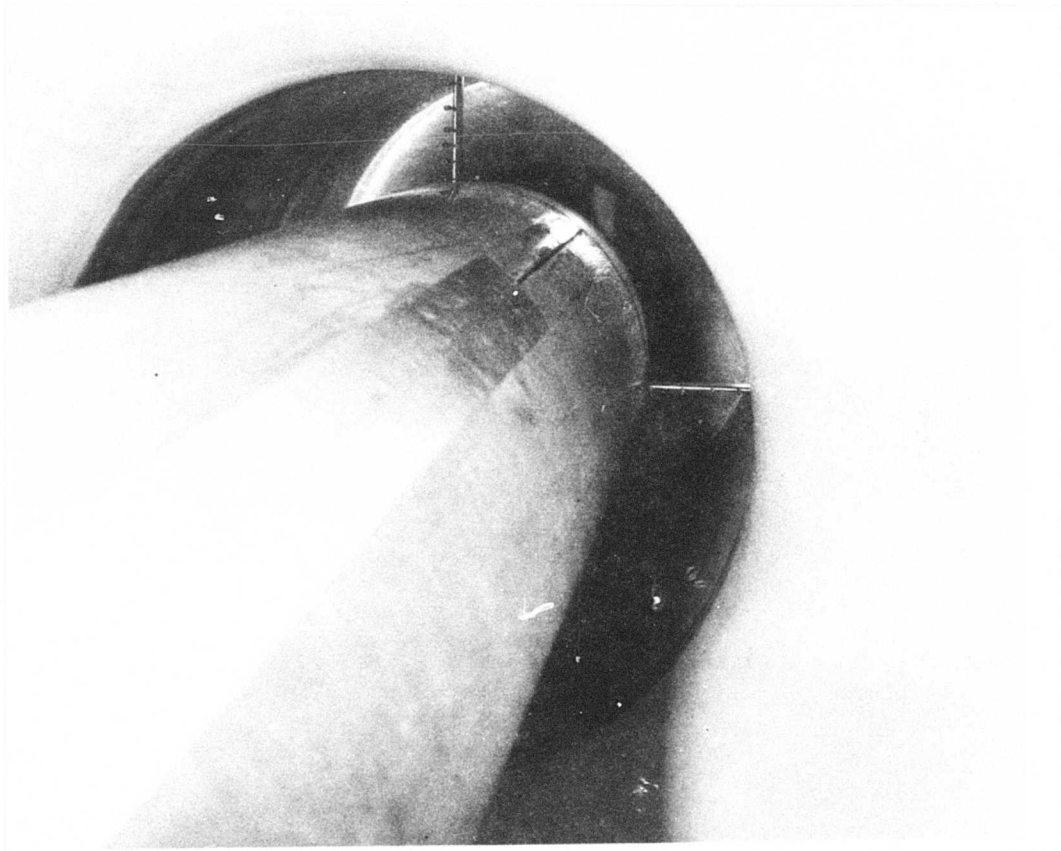

Figure 5.—Secondary Annulus Charging Station Used in Secondary Mass Flow Measurements

2.5 TEST PROCEDURE

Steady state nozzle thrust and mass flow were measured for each test configuration at the hot nozzle test facility. Five one-second-duration, integrated thrust measurement samples were obtained for each test condition to obtain an assessed accuracy of ±0.25%. In order to measure mass flow without perturbing the secondary flow characteristics, the ejector bellmouth was extended by a cylindrical duct and a very large bellmouth, as described in figure 8. Inspection of the body forces and pressure fields near the throat will show that the additional hardware creates a minimum amount of perturbation of the secondary flow. The quantity measured could therefore be applied as well to any bellmouth inlet ejector configuration as tested without the large bellmouth/annulus. Bellmouth and duct were chosen of a sufficient size to allow parallel flow throughout the duct and in the annular measuring station installed therein.

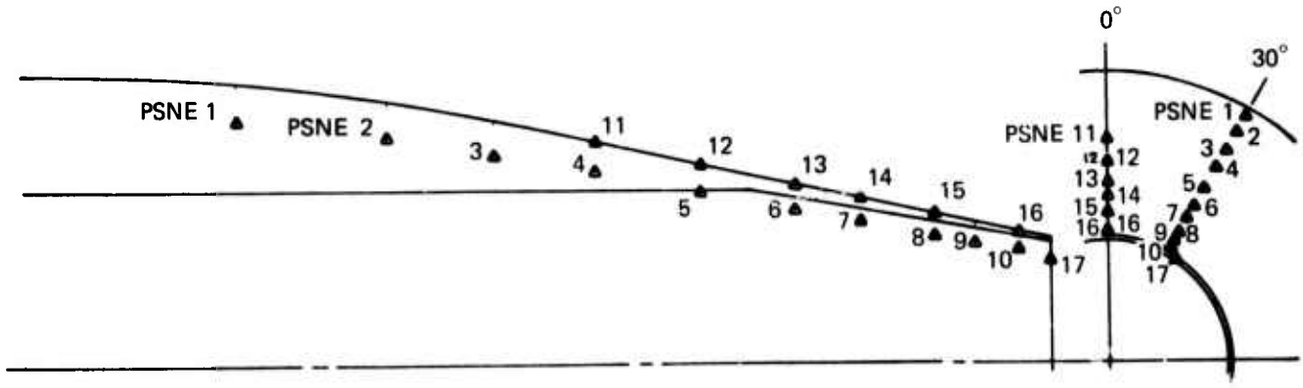

Note: See appendix A for dimensions

Figure 6.—R/C Nozzle Instrumentation (PSNE) (External Static Pressure)

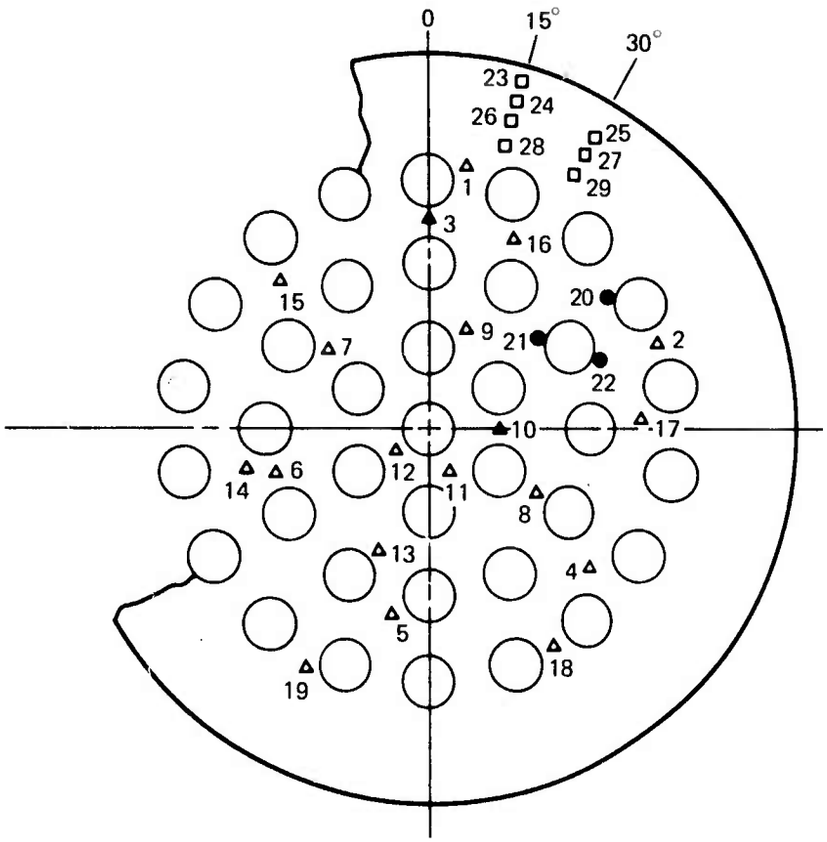

△ PSNE 1-19—baseplate static pressure
● PSNE 20-22—tube exit plane static pressure
□ PSNE 23-29—ramp static pressure

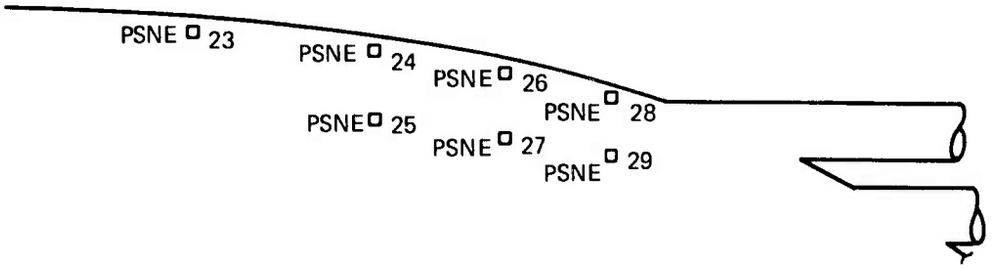

Note: See appendix A for dimensions

Figure 7. R/37 Nozzle Instrumentation (PSNE) (Static Pressure)

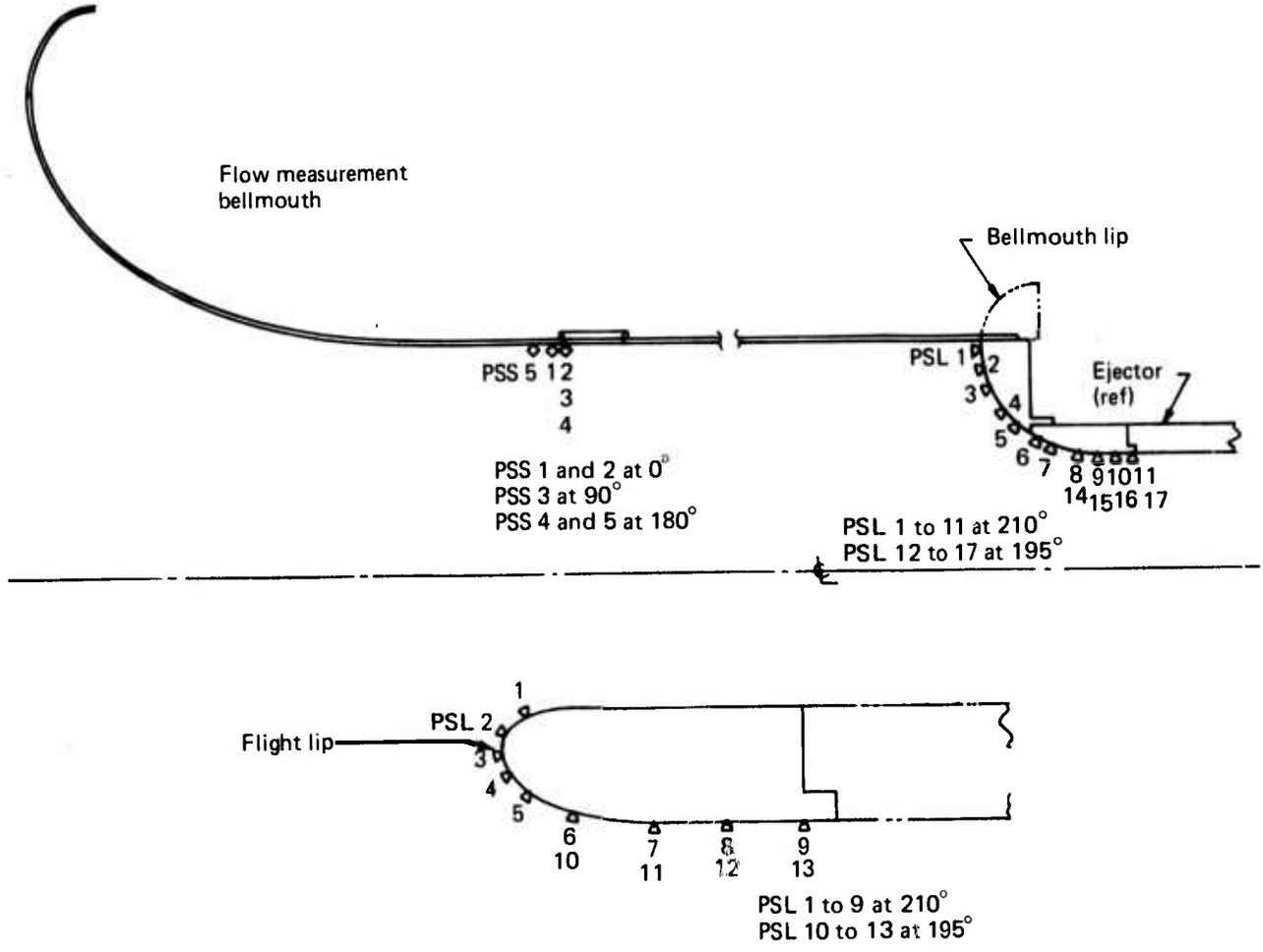

Figure 8.—Ejector Inlet Instrumentation (Static Pressure)

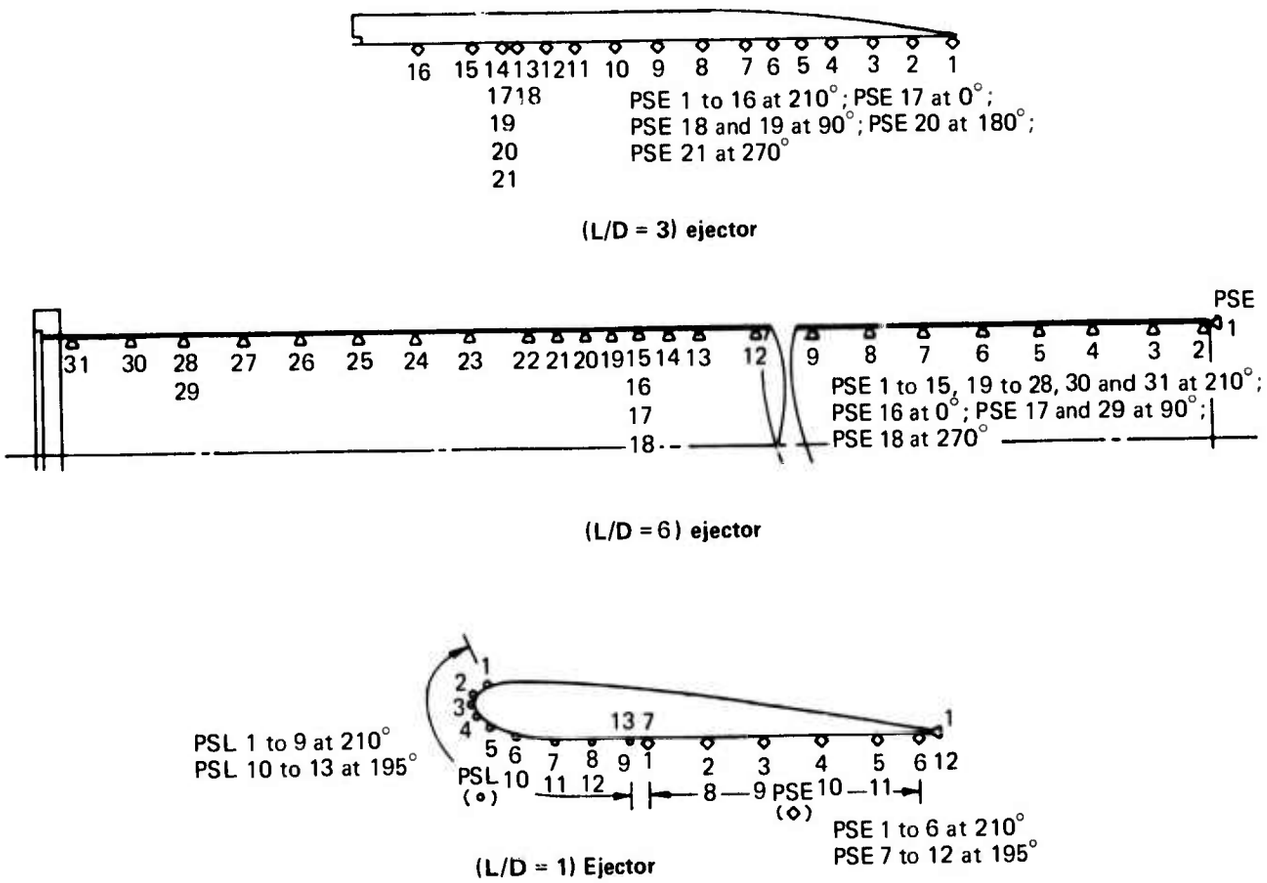

Figure 9.—Ejector Instrumentation (Static Pressure)

3.0 EXPERIMENTAL RESULTS AND ANALYSIS

Thrust and airflow performance were measured for both referee nozzles in primary alone configurations and with ejector shrouds. Nozzle discharge coefficients and gross thrust coefficients from the data were correlated with analytical prediction for the round convergent nozzle and with experimental data obtained for other 37-tube nozzles.

3.1 BARE NOZZLE

3.1.1 DISCHARGE COEFFICIENT

Primary mass flow data were obtained for the majority of the configurations for both cold and hot flows. Discharge coefficients were corrected for temperature effects, resulting in correlations between ambient and high temperature runs. The corrected primary discharge coefficients are plotted in figures 10 and 11 and compared with values predicted from previous tests. The predicted values of C_D for the R/C nozzle were obtained by interpolating from a parametric study (ref. 4). Predictions for the R/37 discharge coefficient were made using previous SST program data (ref. 1).

The experimental data are derived from the average of at least two runs corresponding to an identical configuration. The data scatter for different runs is generally within 0.25%.

3.1.1.1 Cold Flow

For the round convergent nozzle, the discharge coefficient is close to 0.985. Data collected with this same nozzle and the 4° diffuser show a 0.5% loss in discharge coefficient. This is caused by the total pressure loss in the diffuser which is located between the charging station and the test nozzle. For the multitube suppressor nozzle, the discharge coefficient is close to the predicted 0.95. The addition of an ejector did not alter the value of C_D in either case. As shown in figure 10 for R/C configurations and in in figure 11 for R/37, the cold flow discharge coefficient agrees satisfactorily with the predicted values; the variations do not exceed 0.5%.

3.1.1.2 Hot Flow

The corrected discharge coefficient should, in theory, be the same for hot flow as for cold flow when the nozzle thermal growth is taken into account; this is verified in figures 12 and 13. Correlations cannot be expected to be as precise as for cold runs because of the temperature profile produced by the burner since the latter is neither exactly square nor totally time dependent. The temperature correction for C_D should therefore be slightly different from the average temperature of the jet. These differences, however, are not large and the nozzle growth correction is adequate in most cases.

3.1.2 PERFORMANCE

Gross thrust coefficient values were obtained from the measured mass flow and thrust. These values for the bare nozzle configurations were compared with predicted values obtained from

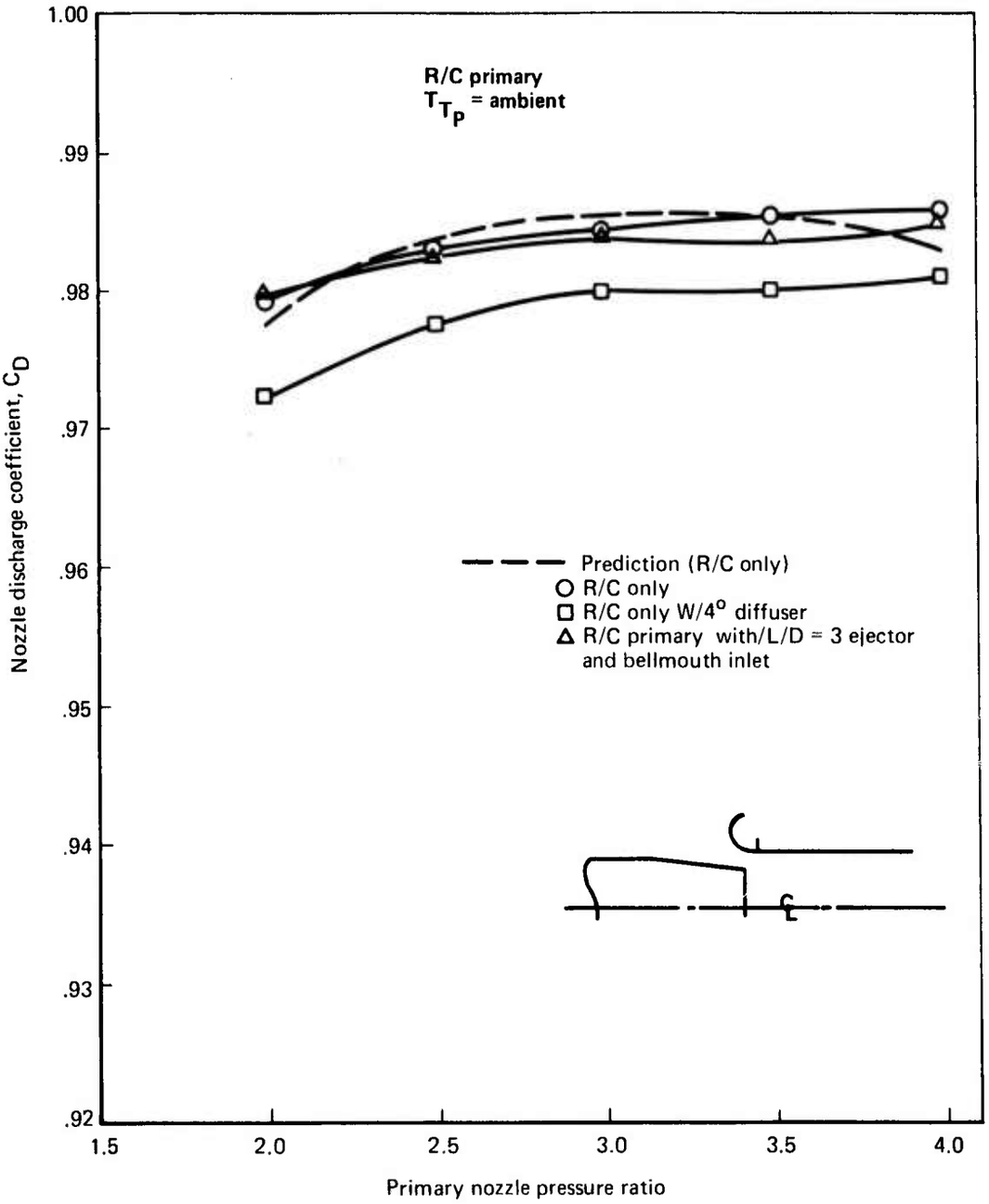

Figure 10.—R/C Nozzle Discharge Coefficient

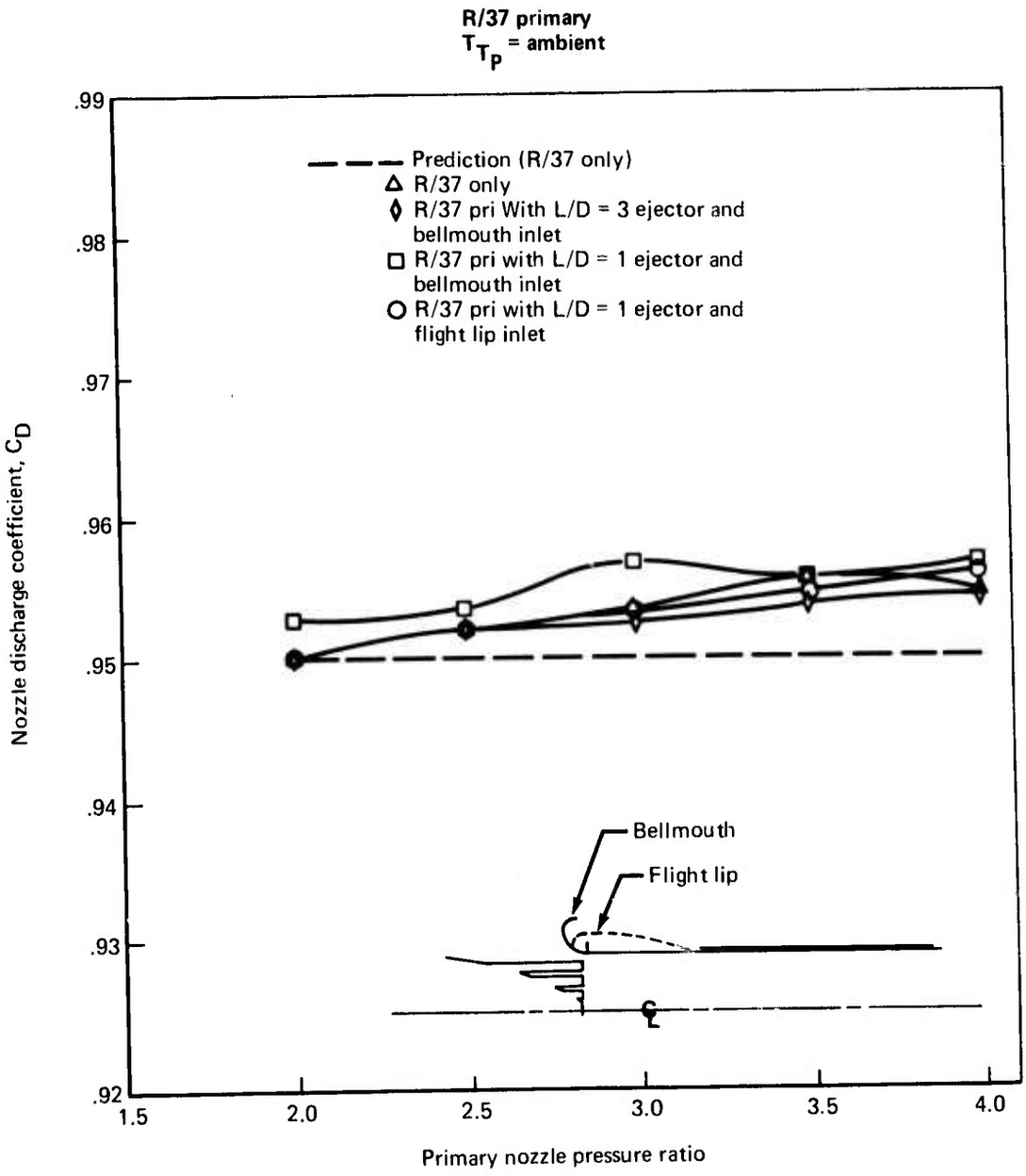

Figure 11.—R/37 Nozzle Discharge Coefficient

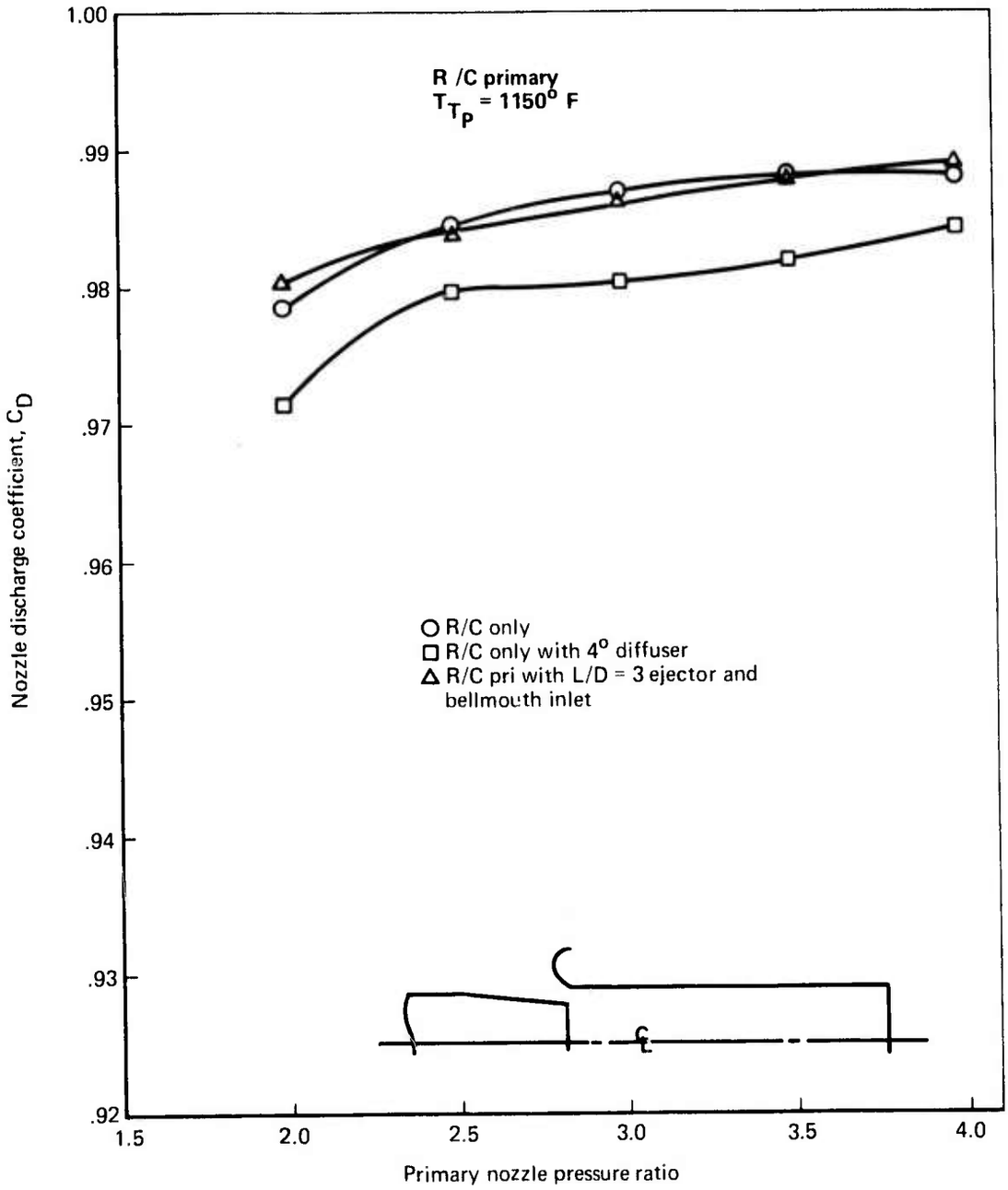

Figure 12.– R/C Nozzle Discharge Coefficient, Hot Primary

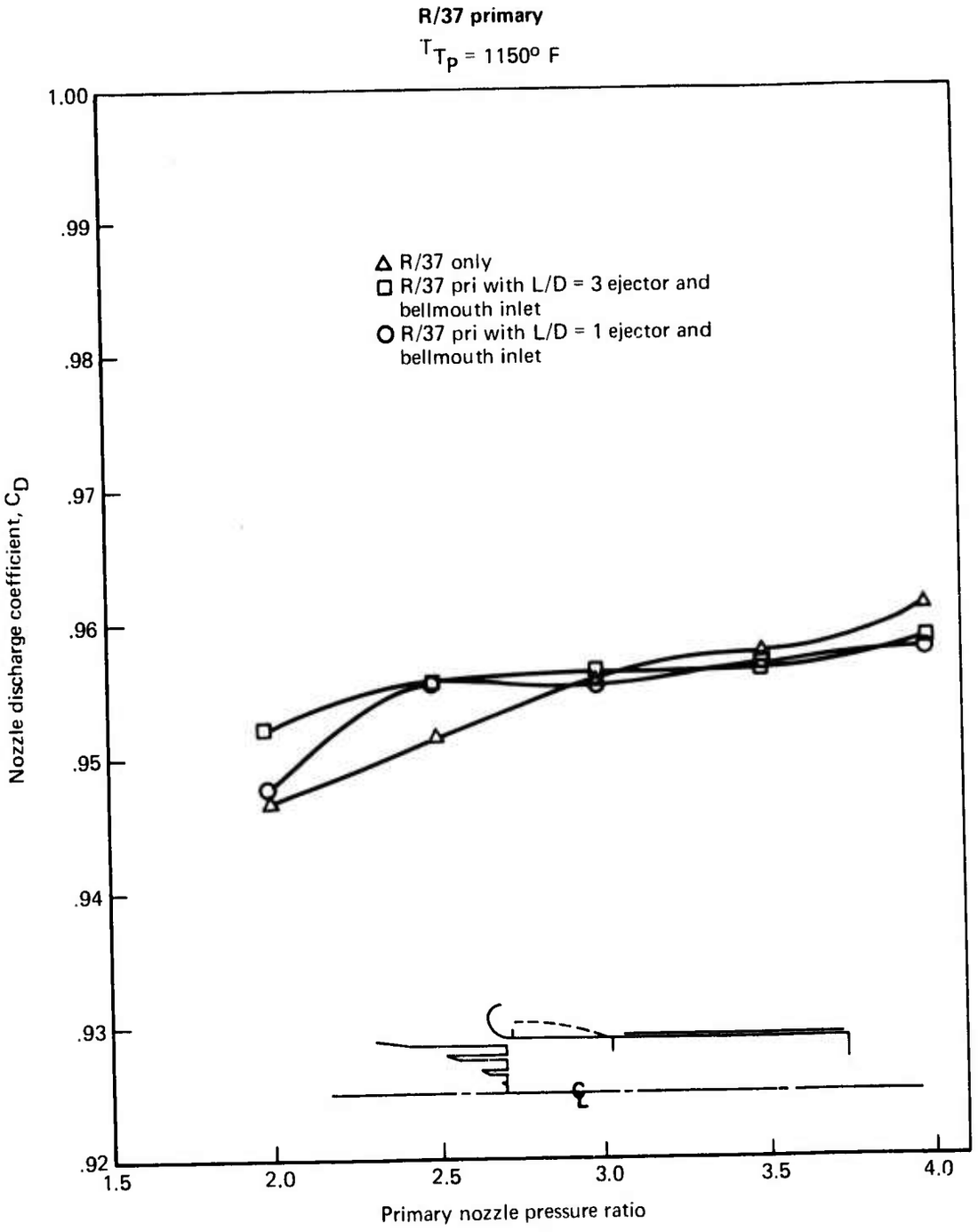

Figure 13.– R/37 Nozzle Discharge Coefficient, Hot Primary

reference 4 for the round convergent nozzle and from reference 5 for the multitube suppressor nozzle. This was done in order to assess the level of accuracy of the measurements performed throughout the test.

Figure 14 shows the gross thrust coefficient for the bare R/C and R/37 nozzles. It indicates that the cold data obtained when testing the round convergent nozzle are within 0.2% of the predicted value. A difference of 0.5% is noticed between tested and predicted C_{FG} for the R/37 nozzle. However, the predicted C_{FG} is obtained for a constant discharge coefficient, and correcting this assumption will narrow the difference between predicted and measured C_{FG} to 0.2% at high pressure ratio. The corrected R/37 cold data match the predictions with 0.2%.

3.2 EJECTOR

Thrust performance was measured for various nozzle ejector configurations. Related nozzle/ejector body forces were determined from pressure measurements. These quantities were plotted as functions of pressure ratio for key configurations for cold flow and hot flow in figures 14 through 23.

The two nozzles were tested with the 3.7 area ratio cylindrical ejectors of various length and inlet shapes. The three ejectors were selected in such a way that comparable fully mixed configurations would be available for either nozzle, i.e., the length over individual jet diameter ratio would be equal to 12 for either ejector configuration (R/C, L/D = 6 and R/37, L/D = 1) and for a partially mixed configuration with the round convergent nozzle (R/C, L/D = 3 ejector) which would be more realistic as far as ejector size is concerned. The inlet of either of these three ejectors could be chosen as a bellmouth-type lip or an elliptical flight-type lip. Thrust measurements were taken for each configuration and the efficiency of each ejector was studied as a function of ejector length and inlet shape.

3.2.1 EJECTOR LENGTH AND NOZZLE CONFIGURATION

3.2.1.1 Performance

The gross thrust coefficients for the nozzle-ejector configurations are plotted in figure 15 for the R/C nozzle and figure 17 for the R/37 nozzle. The data considered here correspond to ejectors fitted with the bellmouth lip. In both figures the nozzle baseline performance is indicated. The addition of an ejector increases the thrust in all cases, as expected, but the amount is a function of the nozzle configuration and ejector length. For the round convergent nozzle, the addition of the L/D = 6 ejector with L/D_{jet} of 12 results in a high increase in thrust, up to 15.3% at low pressure ratios and 6% at high pressure ratios. Similarly, the L/D = 1 ejector fitting onto the multitube nozzle R/37 (L/D_{jet} is also equal to 12 in this case) creates similar thrust increases of 14.6% at low pressure ratio and 7% at high pressure ratio. A more detailed analysis of these ejector/nozzle interactions requires that the measured thrust be broken into its major components: bare nozzle internal thrust; nozzle base or ramp drag; ejector boattail drag and internal drag (both negligible in these configurations); and ejector lip suction. Nozzle base drag and ejector lip suction are plotted in figure 16 for the R/C nozzle with L/D = 6 and L/D = 3 ejectors and in figure 17 for the R/37 with an L/D = 1 ejector.

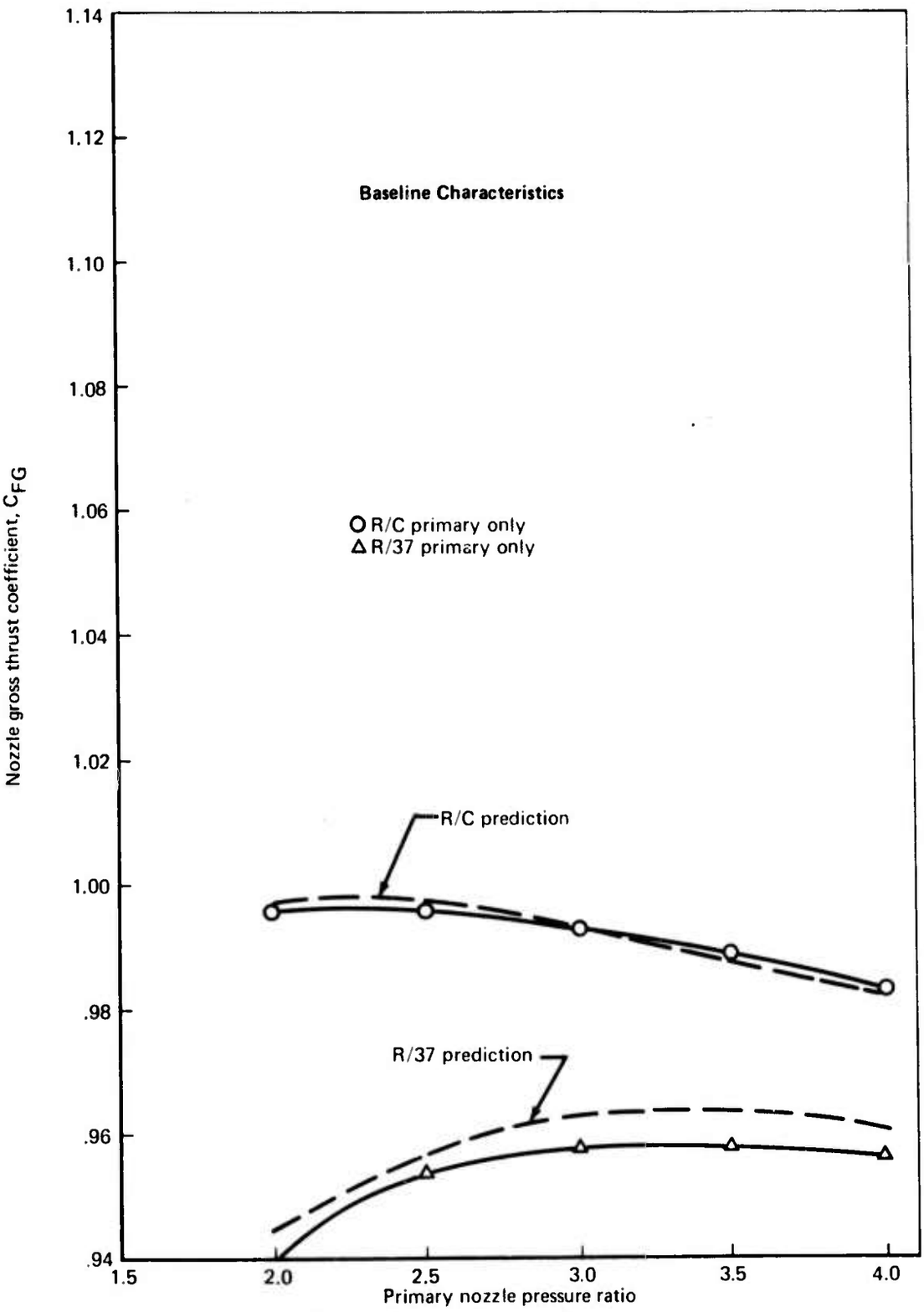

Figure 14.—Bare Nozzle Performance

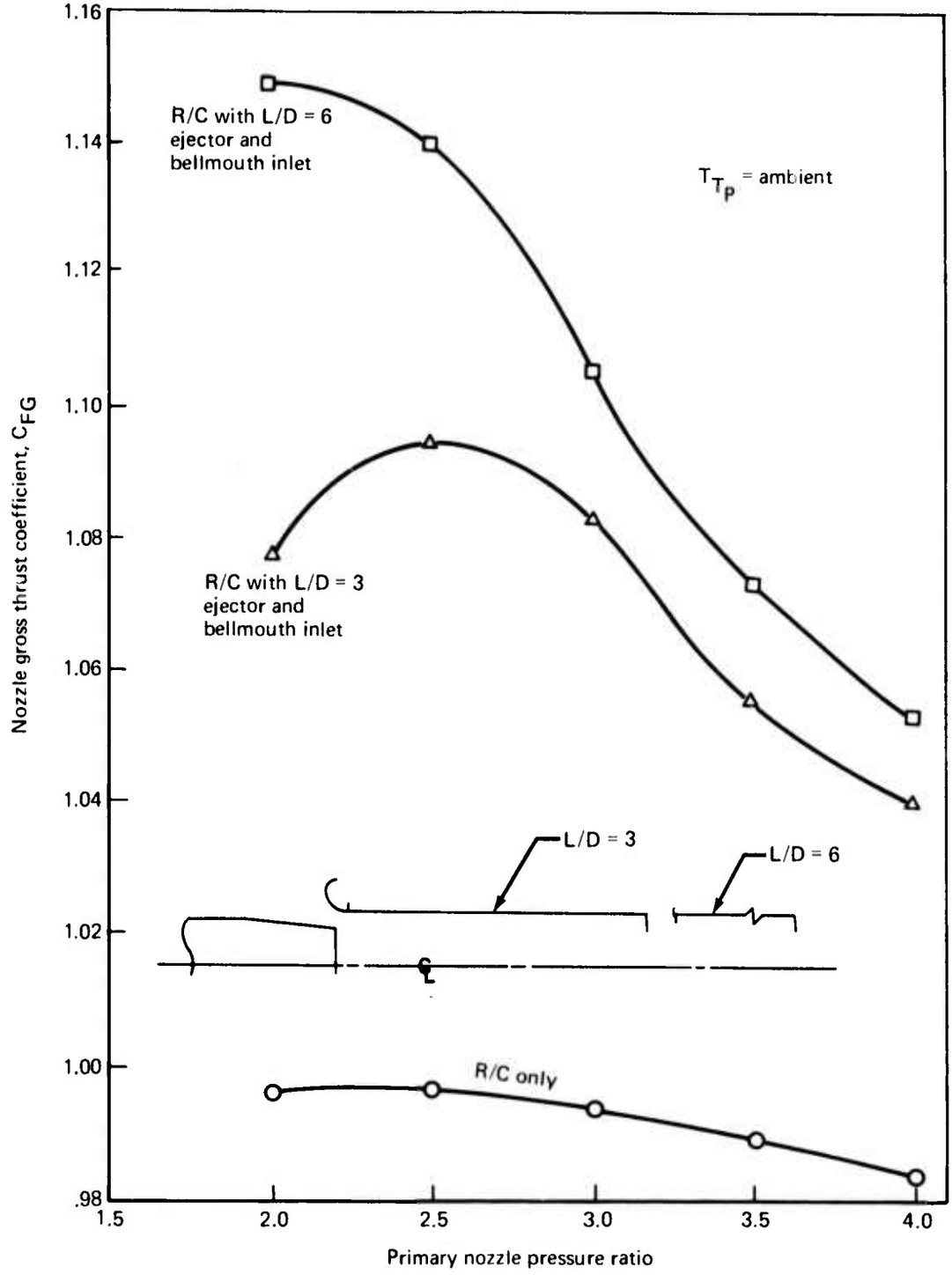

Figure 15.—Effect of Ejector Length on R/C Performance

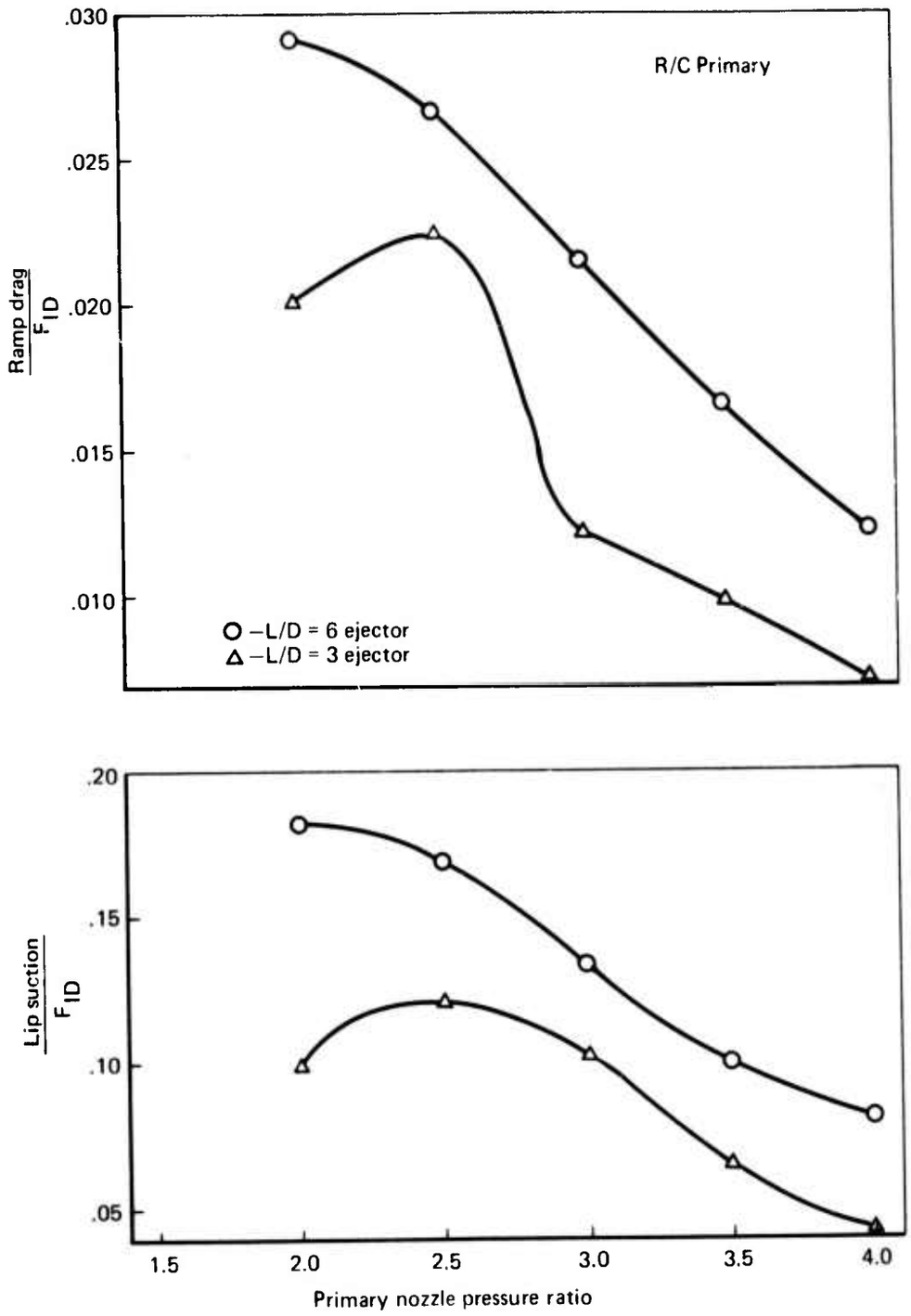

Figure 16.—Effect of Ejector Length on R/C Configuration Body Forces

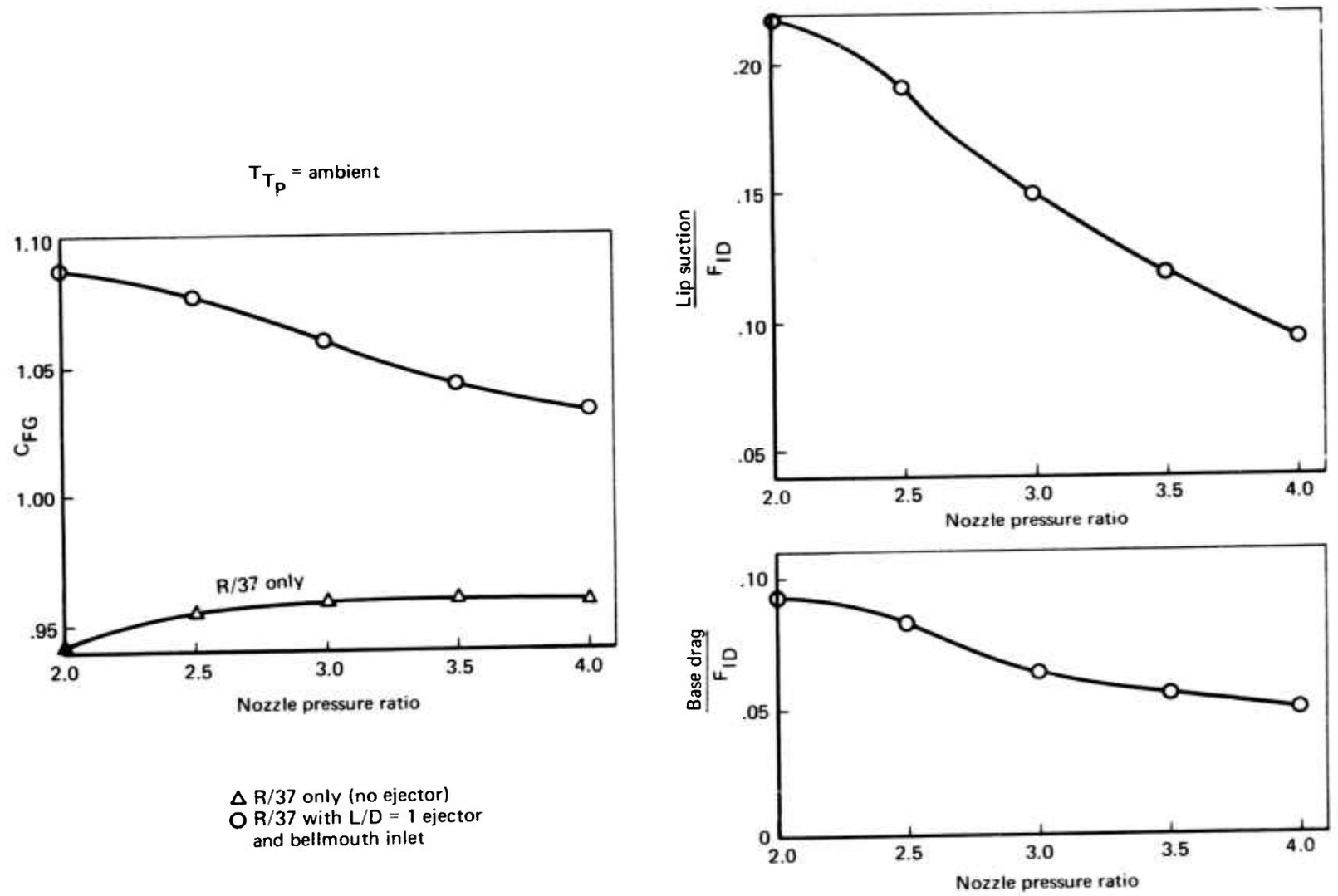

Figure 17.—Effect of Ejector Addition on Performance and Body Forces, R/37 Nozzle

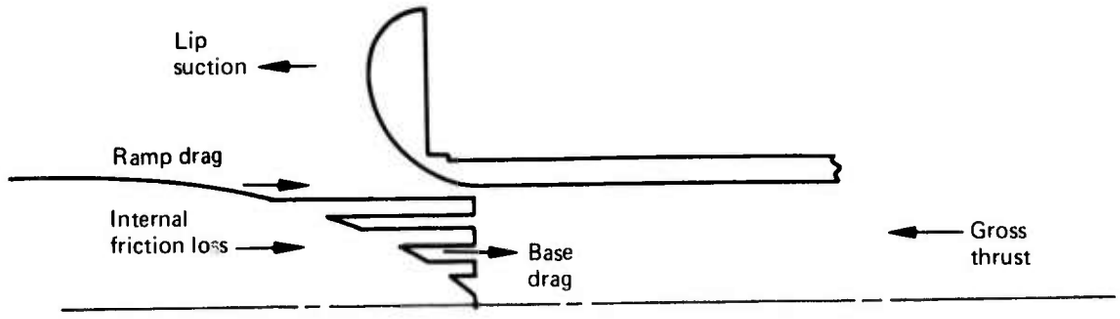

Figure 18.–Ejector/Nozzle Component Forces

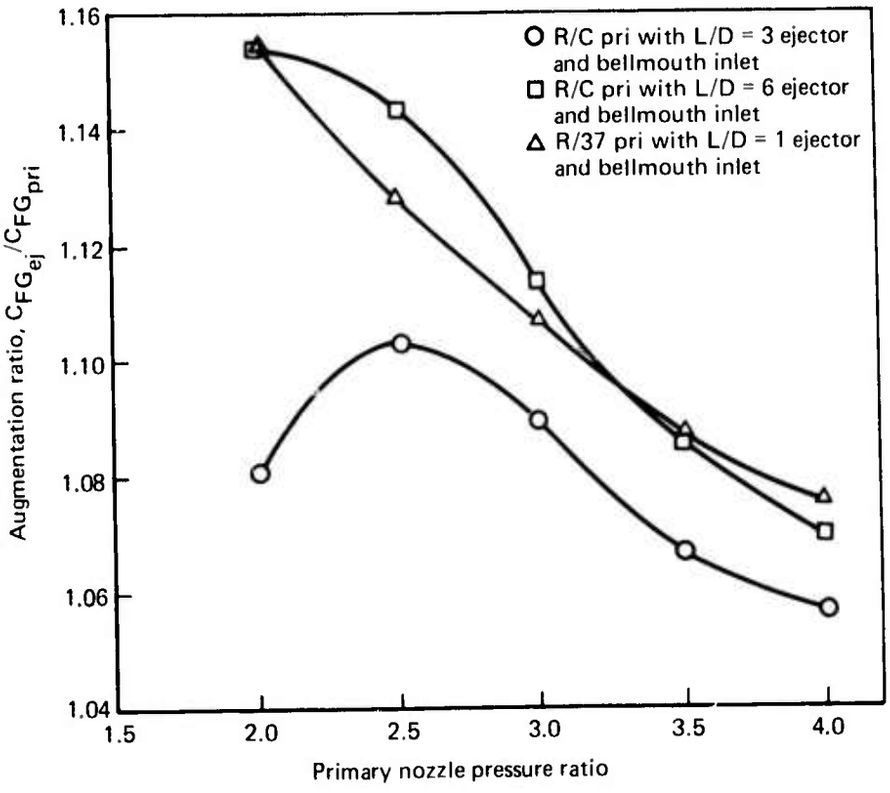

Figure 19.–Ejector Efficiency

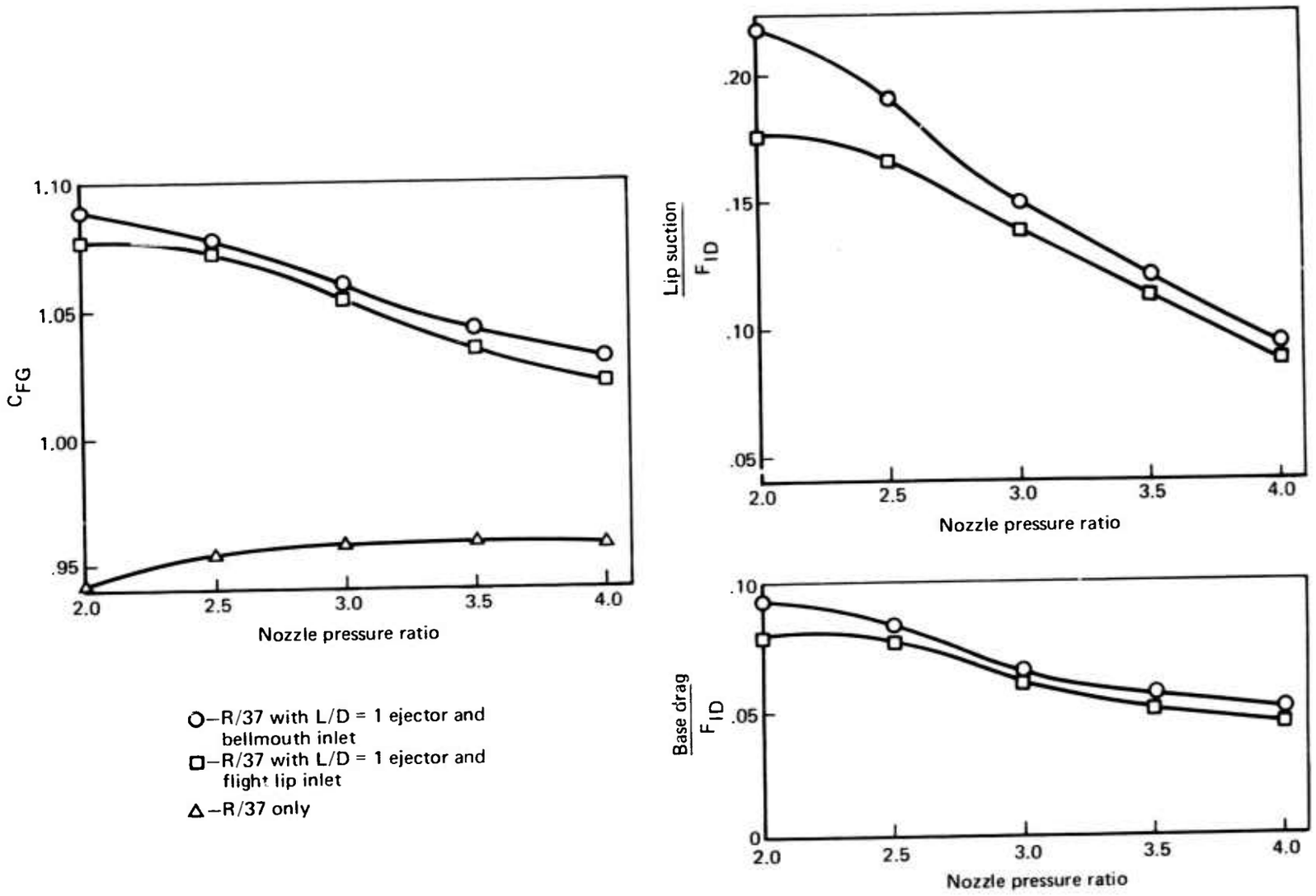

Figure 20.—Effect of Ejector Inlet Change on R/37 Configuration

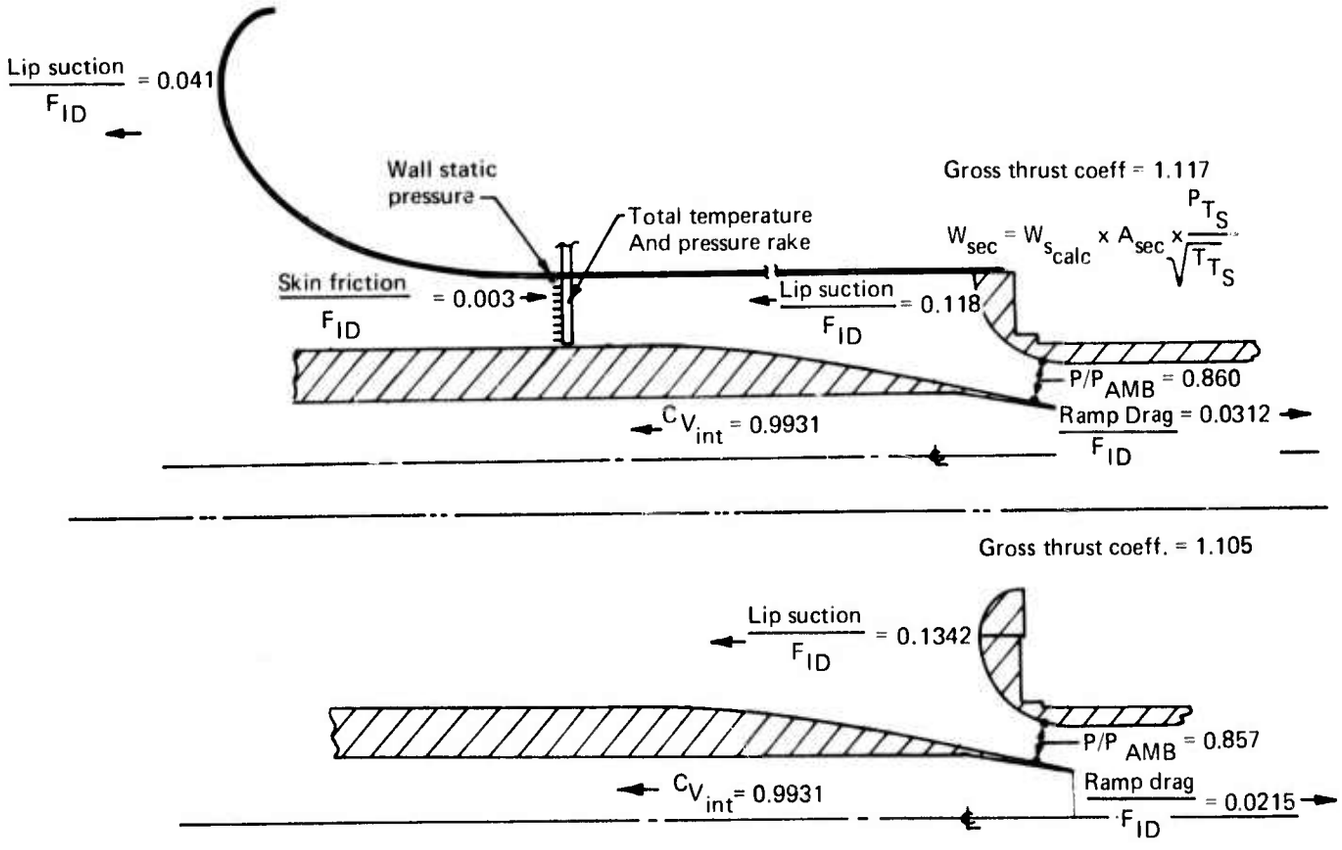

Figure 21.–Ejector Nozzle Body Forces and Secondary Mass Flow Measurements

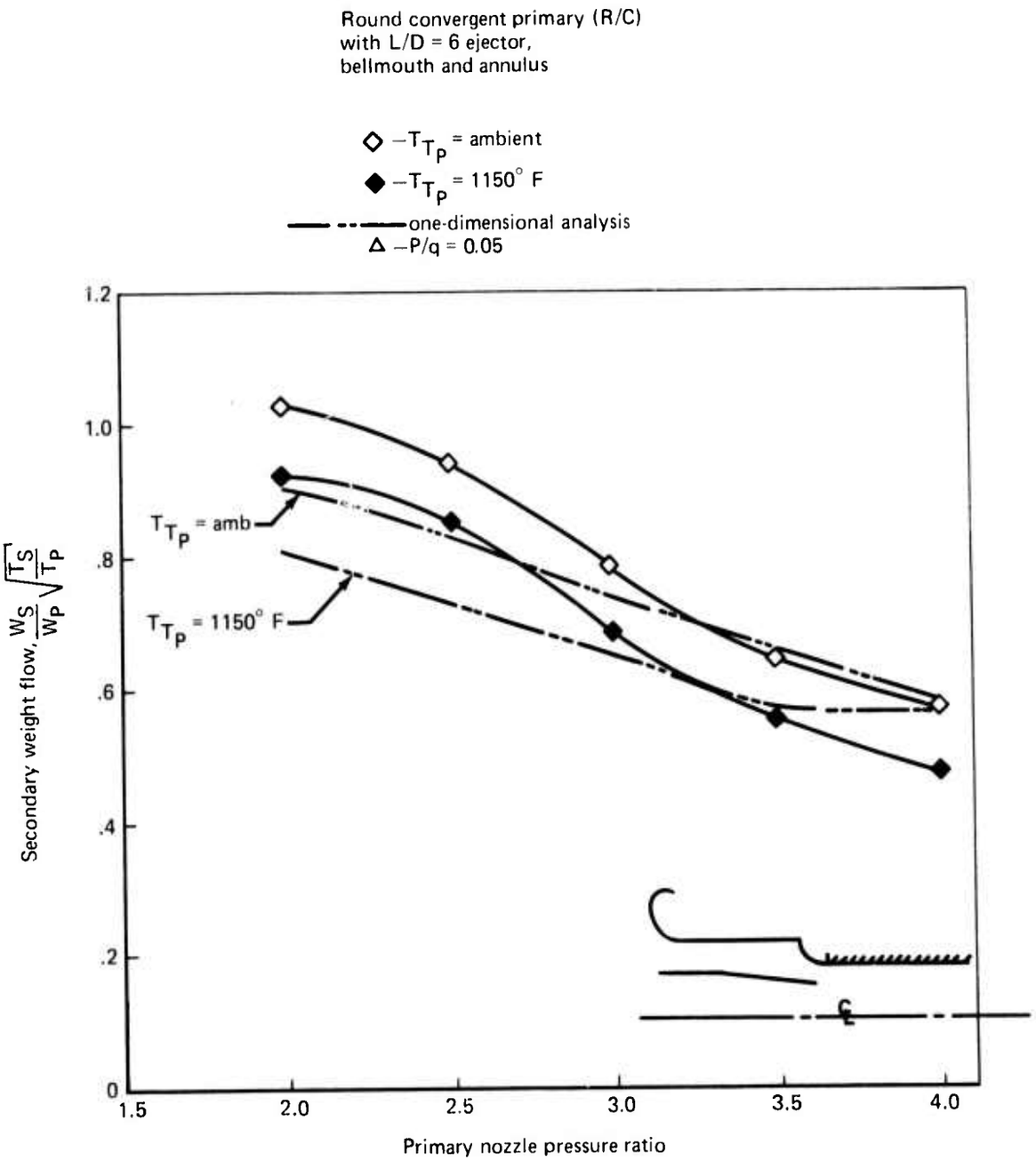

Figure 22.—Secondary Mass Flow for a Fully Mixed R/C Configuration

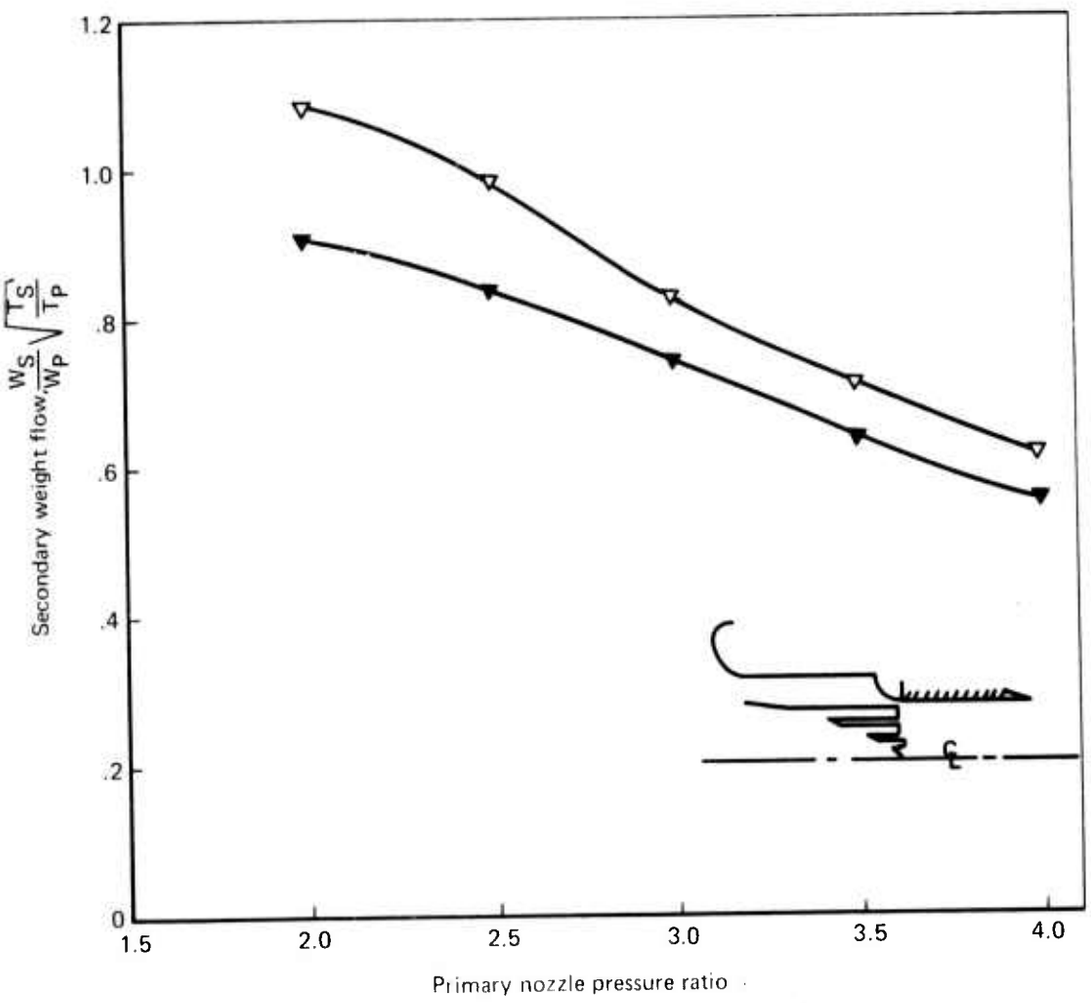

Figure 23.—Secondary Mass Flow for a Fully Mixed Multi Tube Nozzle

3.2.1.2 Body Forces

A correlation of measured gross thrust and ejector/nozzle component forces is illustrated in figure 18.

Drag and suction forces are calculated from measured static pressures and provide independent means of obtaining the gross thrust coefficient. The internal thrust of the bare nozzle is obtained by subtracting all exterior drag from the measured thrust, i.e., ramp drag for the R/C nozzle and base drag for R/37. The ramp drag for the R/C case is very small and can be neglected. The base drag for R/37 alone was calculated from static pressure measurements. The difference in internal thrust between both nozzles is caused by the loss associated with the increased wetted area of the multitube nozzle and amounts to approximately 3% at PR = 2.0.

Nozzle drag forces during tests with ejectors were a ramp drag of approximately 3% at pressure ratio 2 for the R/C and base drag of up to 9% of ideal nozzle thrust for the R/37 nozzle.

Ejector lip suction is quite large for both configurations—up to 22% for the R/37 with L/D = 1 ejector at PR of 2.0— and represents the major factor of thrust increase. Depending on the nozzle, however, small differences can be noticed: for example, the lip suction coefficient for R/C configurations is smaller by about 3.5% at PR of 2.0. A short calculation combining all the above body forces yields at PR of 2.0 an increase of 14.76% above the base R/37 nozzle for the R/37 with L/D = 1 ejector gross thrust coefficient, and similarly, a 15.31% increase for R/C with L/D = 6 ejector.

The ejector augmentation ratio (C_{FG} ejector)/(C_{FG} primary) is compared for the various nozzle-ejector configurations as a function of pressure ratio in figure 19. As expected, the R/C, L/D = 6 ejector and R/37, L/D = 1 ejector show similar results to those derived from pressure measurements (body forces) and match the one-dimensional theory for the R/C nozzle when accounting for an ejector inlet loss.

$$\frac{\Delta P_T}{q} = 0.05$$

When the L/D = 3 ejector is used with the round convergent nozzle, a smaller augmentation ratio results than for either fully mixed case (between 2% or 3% smaller at all pressure ratios, except PR of 2.0 where the difference is much larger).

3.2.2 EJECTOR INLET

The ejector inlet can be chosen with a bellmouth-type lip or with an elliptical flight lip. In order to measure the secondary mass flow, the small bellmouth is extended by a cylindrical duct and a larger bellmouth. The lips are designed so that the secondary geometric throat area is kept constant. The lip suction plays a major part in the thrust augmentation provided by an ejector; the ejector and the ramp and base drags are expected to be a function of the flow velocity and, therefore, of the inlet shape. Thrust coefficients have been calculated and surface static pressures have been recorded for the major configurations. This information can now be compared.

The nozzle considered in this section is the multitube suppressor nozzle R/37 with the L/D = 1 ejector. In figure 20 the gross thrust coefficients are plotted for the ejector with a bellmouth lip and with a flight lip. Also shown are lip suction and nozzle base drags computed from surface pressure measurements. From the figure, it appears that the bellmouth lip provided between 0.5% and 1% more thrust than the flight lip. This is expected when considering the theoretical air intake efficiency calculated in reference 6 for the two lips. (This efficiency is close to 98.5% for the bellmouth lip and 96.5% for the flight lip inlet.) The difference in inlet efficiency is also seen to affect nozzle base drag (in the case of the R/37, i.e., with the gently sloping base), by a small amount. Base drag (percent of gross thrust) would be more strongly affected by nozzle configuration when the nozzle elements (tubes) are mounted in a flat base plate.

3.3 EJECTOR FLOW

3.3.1 SECONDARY MASS FLOW MEASUREMENT

The amount of air entrained into the ejector by the primary jet directly affects the performance of the ejector/nozzle configuration and is related to the flow characteristics near the secondary inlet. The secondary flow rate has a direct influence upon the ejector lip suction, and as a result the nozzle base or ramp drag influences the gross thrust. Measurement of secondary flow allows calculation of flow momentum, and in combination with body forces determined from pressure measurements, allows for direct correlation with measured thrust performance.

In order to measure the secondary flow, the bellmouth is extended by a cylindrical duct and a very large bellmouth, as described in figure 7. The annular measuring station is instrumented with total temperature and pressure probes. The secondary flow rate is calculated through combining average measured total pressures and temperatures with a mass flow coefficient obtained analytically by using a potential flow-boundary layer interaction method (ref. 3).

$$W_S = C_{W_{S(\text{calculated})}} \times \text{geometric area} \times \frac{P_{T_S}}{\sqrt{T_{T_S}}}$$

Total pressures and temperatures are measured within the annular secondary measuring station with area weighted probes. An average value is then calculated and used in the above formula.

In the analysis, a potential flow numerical solution for the configuration specified in the input is first calculated; the effect of the boundary layer growth is then determined by displacing the original body surface by the appropriate amount. The mass flow coefficient is obtained when a given potential flow calculation produces the same boundary layer that was assumed for the potential flow solution. In the mass flow determination, the geometry of the system is first input and then the flow rate coefficient is calculated per above as a function of the wall static pressure of the secondary charging station. The geometric secondary flow area is introduced in the calculation as a constant $A_S = 139.97$ in^2.

It can be assumed that the addition of the cylindrical duct and large bellmouth did not modify the flow at the throat of the secondary inlet and that this flow rate would also be valid for a regular bellmouth inlet configuration. This assumption was checked by comparing the forces on both inlets and the pressure fields in the vicinity of the throat (see fig. 21).

The forces involved include the nozzle ramp or base drag, the lip suction and the large bellmouth suction, and a skin friction. An inspection of the values calculated for these forces shows the following trends when adding the large bellmouth: the lip suction is decreased, the base drag or ramp drag is increased by a small amount, there is a lip suction from the large bellmouth, and the related skin friction L/D = 1 ejector at pressure ratio of 2.0. The lip suction coefficient is decreased by 0.033, the base drag coefficient is increased by 0.004, and the large bellmouth provides a lip suction coefficient of 0.03. The total difference in gross thrust coefficient when adding the large bellmouth is on the order of 0.001. This difference shows that the thrust of the system has not been noticeably modified by the addition of the bellmouth annulus.

Compare the selected static pressure taps along the nozzle ramp or base, on the ejector lip, and on the wall of the ejector close to the inlet. For the round convergent nozzle configurations, the static pressure taps closest to the secondary throat (minimum inlet flow area) are probe 10 on the nozzle ramp and probe 8 on the lip. The static pressure indicated by the average of these two probe measurements is the best available representation of the secondary flow pattern. Changes in this average pressure are indicative of changes in secondary mass flow. However, since the static pressure gradient across the throat is not known, it is not certain that this average pressure is indicative of the average secondary Mach number.

For the round convergent nozzle with the L/D = 3 and L/D = 6 ejectors the following pressures are obtained as shown in table 1.

Table 1.—Ejector throat Static Pressure Variation

PR	Average throat static P_{AMB}
	L/D = 3:
2.0	-0.005
2.5	-0.0045
3.0	+0.0020
3.5	-0.0015
4.0	-0.0015
	L/D = 6:
2.0	+0.004
2.5	+0.005
3.0	+0.0035
3.5	+0.0025
4.0	+0.004

Note: Plus sign indicates a pressure increase when adding the large bellmouth.

A variation of pressure ratio on the order of ±0.005 results, at most, in a change in Mach number of 0.01, and this indicates the magnitude of the error that could be made in the mass flow measurement relative to the small bellmouth configuration: error in W_S = ±0.5%. A summary of the body force and static pressure variations between the two configurations is shown in figure 21.

A check of the ejector wall static pressures close to the secondary inlet indicates a variation in pressure ratio of the same order of magnitude (see figs. 24 and 25).

Since only minor changes to the flow characteristics and body forces are introduced by the addition of the large bellmouth-annulus setup and because those changes can be corrected easily if the large bellmouth is sufficiently instrumented, this method for measuring the secondary mass flow is reasonably accurate.

3.3.2 EJECTOR SECONDARY AIR HANDLING CHARACTERISTICS

The amount of secondary air entrained is very similar for the multitube suppressor nozzle with L/D = 1 ejector and for the round convergent nozzle with the L/D = 6 ejector, the maximum difference being on the order of 3% and occurring at high pressure ratio. For the partial mixing configuration, R/C with L/D = 3 ejector, approximately 20% less air is entrained into the ejector by the primary jet; the maximum flow rate for this configuration occurs at PR = 2.5, which can be correlated with the gross thrust coefficient for the same conditions.

The amount of secondary air entrained per unit of primary mass flow (flow rate augmentation ratio) is most representative of the flow characteristics. It can be corrected for temperature effects by introducing a temperature square root term and is plotted as

$$\frac{W_S}{W_P}\sqrt{\frac{T_{T_S}}{T_{T_P}}}$$

in figures 22 and 23 for the configurations mentioned above. The mass flow augmentation ratio for both the round convergent nozzle with L/D = 6 ejector and the multitube nozzle with L/D = 1 ejector is of the same order of magnitude. It is slightly higher for the multitube nozzle by approximately 3%, indicating that the suppressor nozzle draws more air in a full mixing configuration than the round convergent nozzle. This can be explained by the differences in hardware configuration between the two nozzles, the multitube nozzle allowing for more air to be entrained around the individual primary jets because of the large "wetted" area of the latter.

For the round convergent nozzle with L/D = 3 ejector, the mass flow augmentation ratio is lower by 10% to 20%, depending on the pressure ratio. This is related to the incomplete mixing phenomenon.

3.4 HOT PRIMARY JET FLOW

With the primary flow heated to a temperature of T_{T_P} = 1150° F gross thrust coefficient and external force measurements were taken for most configurations. These results were compared with those at ambient temperature.

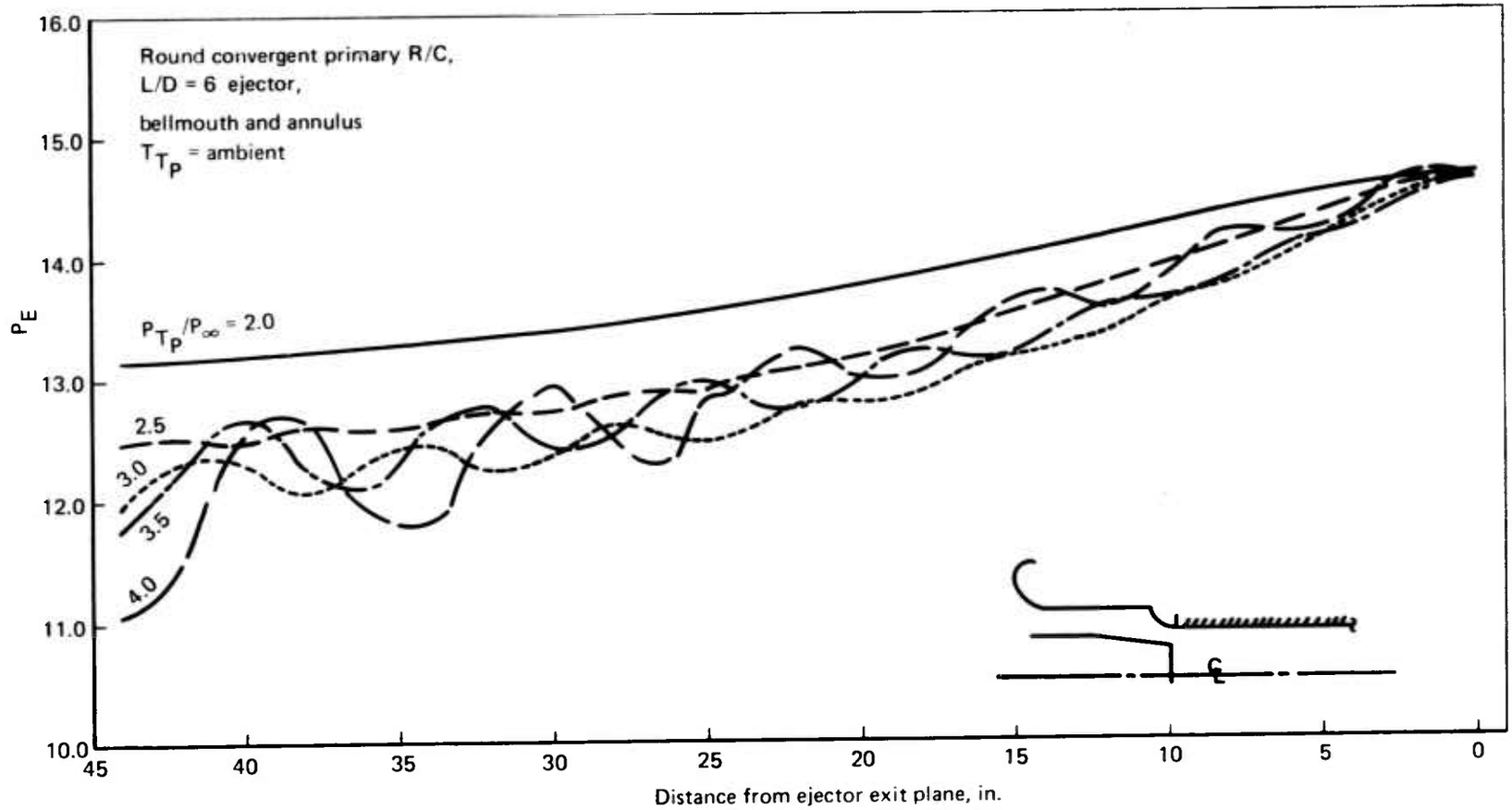

Figure 24.—Ejector Wall Static Pressures for a Fully Mixed R/C Configuration

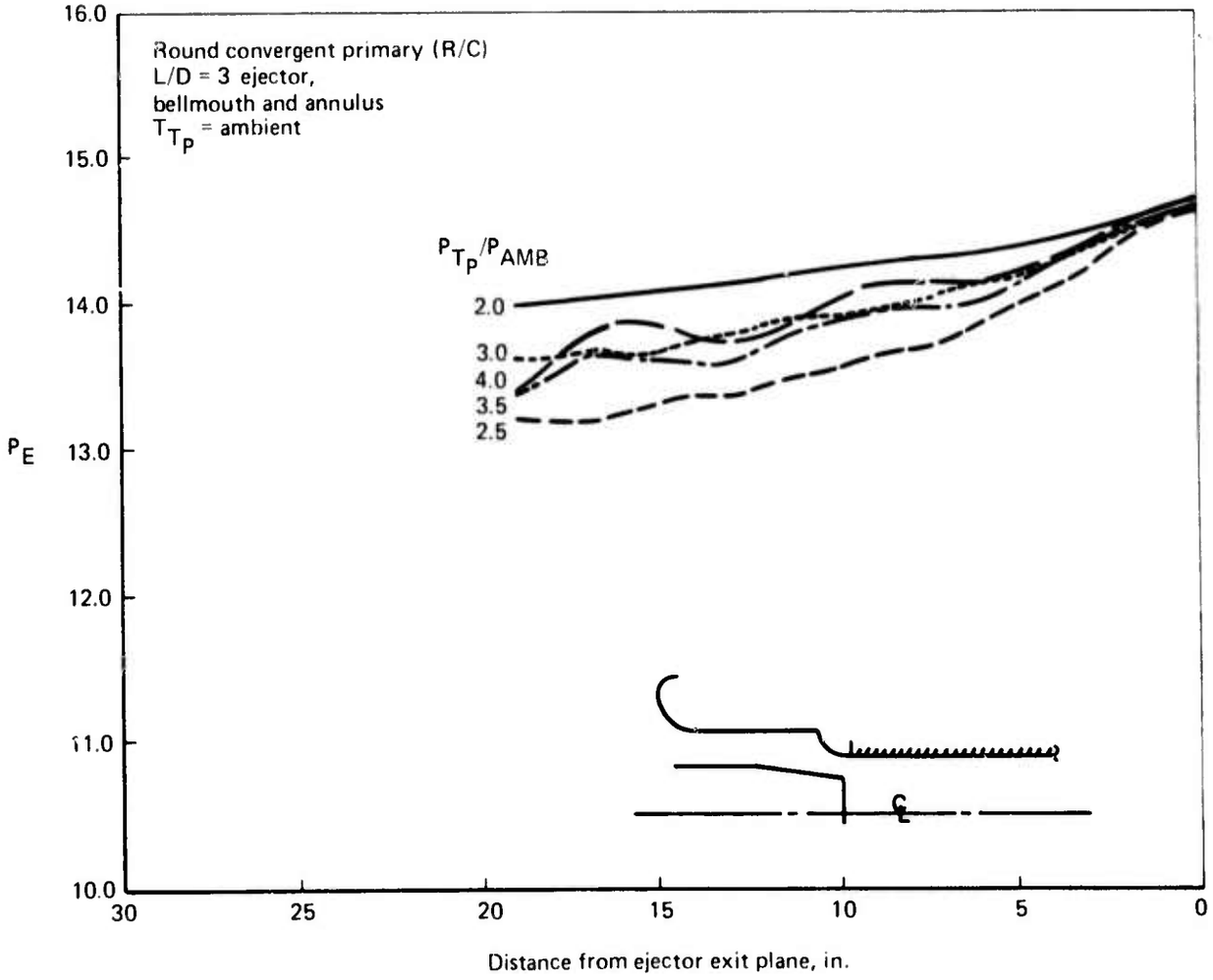

Figure 25.—Ejector Wall Static Pressures Partially Mixed R/C Configuration

3.4.1 BARE NOZZLE

For a round convergent nozzle, the internal velocity coefficient can be approximated by the following first order equation:

$$C_{V_{int}} = 1 - \frac{2\theta}{r}$$

where θ is the momentum thickness of the turbulent boundary layer and is directly proportional to a power of the Reynolds number; r is the exit radius of the nozzle.

For a cold flow, the Reynolds number per unit length is equal to 0.32×10^6 ft^{-1} (standard sea level day). When the flow is heated, the Reynolds number decreases; for example, at T_{T_p} = 1150° F, Re = 0.082×10^6 ft^{-1}. The momentum thickness varies proportionately to the Reynolds number, so that

$$\frac{\theta \text{ cold}}{\theta \text{ hot}} = \left(\frac{Re_{cold}}{Re_{hot}}\right)^{\frac{1}{5}} \sim 0.762$$

This induces a small internal velocity coefficient variation with temperature and, as external forces on a bare R/C nozzle are negligible, a small variation of the gross thrust coefficient, for example:

PR	2.0	2.5	3.0	3.5	4.0
C_{FG}cold	0.9958	0.9963	0.9931	0.9985	0.9834
C_{FG}hot	0.9948	0.9955	0.9913	0.9852	0.9786

estimated at T_{T_p} = 1150° F.

The nozzle radius and the boundary layer growth are affected by temperature. The former, however, can be neglected as it changes by a very small amount while the momentum thickness variation amounts to 20%

The internal velocity coefficient for the multitube nozzle can be written

$$C_{V_{int}} = 1 - \frac{2\theta}{r \text{ equivalent}} \times \frac{\text{Multitube nozzle perimeter}}{\text{Equivalent R/C nozzle perimeter}}$$

where θ ,the boundary layer momentum thickness, is proportional to the one-fifth power of the Reynolds number.

The variations of $^{C}V_{int}$ with temperature are calculated for the R/37 nozzle; $^{C}V_{int}$ for hot runs (1150°F) is lower than for cold runs by up to 1%.

In the case of the bare R/37 nozzle the external forces consist mainly of the base drag, which has been experimentally shown to vary with temperature. When the flow is heated to 1150°F, the base drag coefficient is lower than the cold flow base drag coefficient:

	PR	2.0	2.5	3.0	3.5	4.0
T_{T_P} = 1150°F	$\frac{DB}{F_{ID}}$	0.0155	0.0130	0.0113	0.0103	0.0026
T_{T_P} = AMB	$\frac{DB}{F_{ID}}$	0.0211	0.0187	0.0171	0.0160	0.0158

The gross thrust coefficient varies with temperature as follows:

	PR	2.0	2.5	3.0	3.5	4.0
C_{FG} cold		0.9417	0.9544	0.9579	0.9595	0.9575

Therefore, a small decrease in bare nozzle gross thrust coefficient (on the order of 0.2% to 0.3%) is expected for the R/37 as well as the R/C nozzle where the primary flow is heated to 1150°F. The gross thrust coefficients obtained experimentally at T_{T_P} = 1150°F for the round convergent nozzle are within 0.35% of the values estimated above and those for the multitube nozzle are within 0.6%. (See fig. 26.)

3.4.2 EJECTOR

By inspecting the hot flow data taken during this test and during parametric testing of various suppressor-ejector configurations, it appears that the thrust and the body forces—mainly the lip suction in the case of R/37—are extremely sensitive to hardware geometry. For example, the position of the ejector inlet relative to the nozzle exit plane, termed "ejector set-back," is an important parameter where gross thrust is concerned. Upon heating of the primary flow, some hardware expansion occurs, and care must be taken to ensure that such geometric factors are considered and that their variations are accounted for.

This section will consider the addition of the L/D = 1 ejector to the multitube suppressor nozzle R/37 for a primary flow at 1150°F. Effect of temperature on gross thrust and body forces will be considered and extended to other cases such as on R/C nozzle with a partially mixed L/D = 3 ejector.

- Temperature effects on thrust performance
  The effect of primary jet temperature on gross thrust coefficients for the R/37 with L/D = 1 ejector configuration is plotted in figure 27. Nozzle base drag and ejector lip suction changes are also indicated. Heating the primary jet reduces thrust performance by a relatively large amount (around 5% at PR at 3.0). Both base drag and lip suction are sensitive to jet temperature and substantially account for the measured thrust difference.

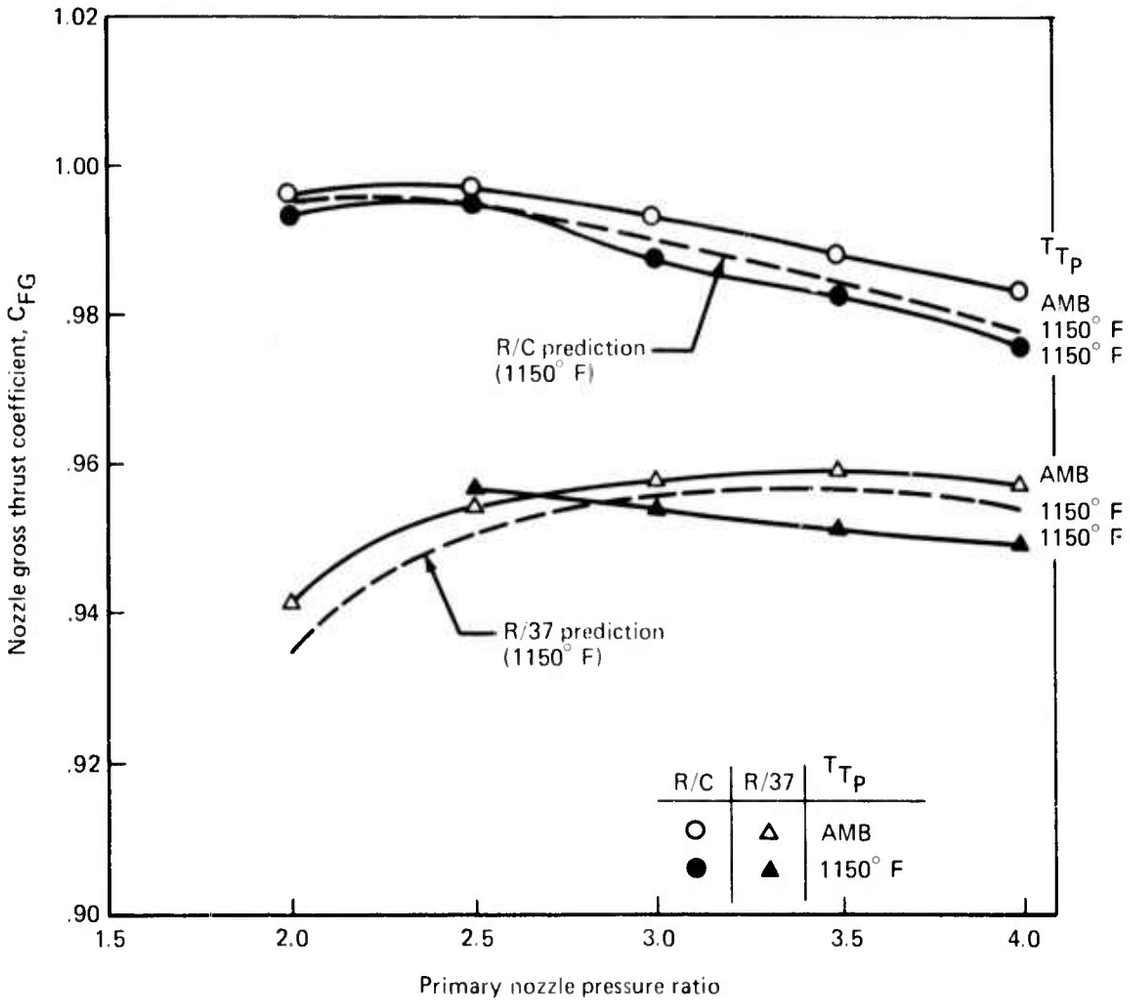

Figure 26. – Bare Nozzles Characteristics, Cold Primary and Hot Primary

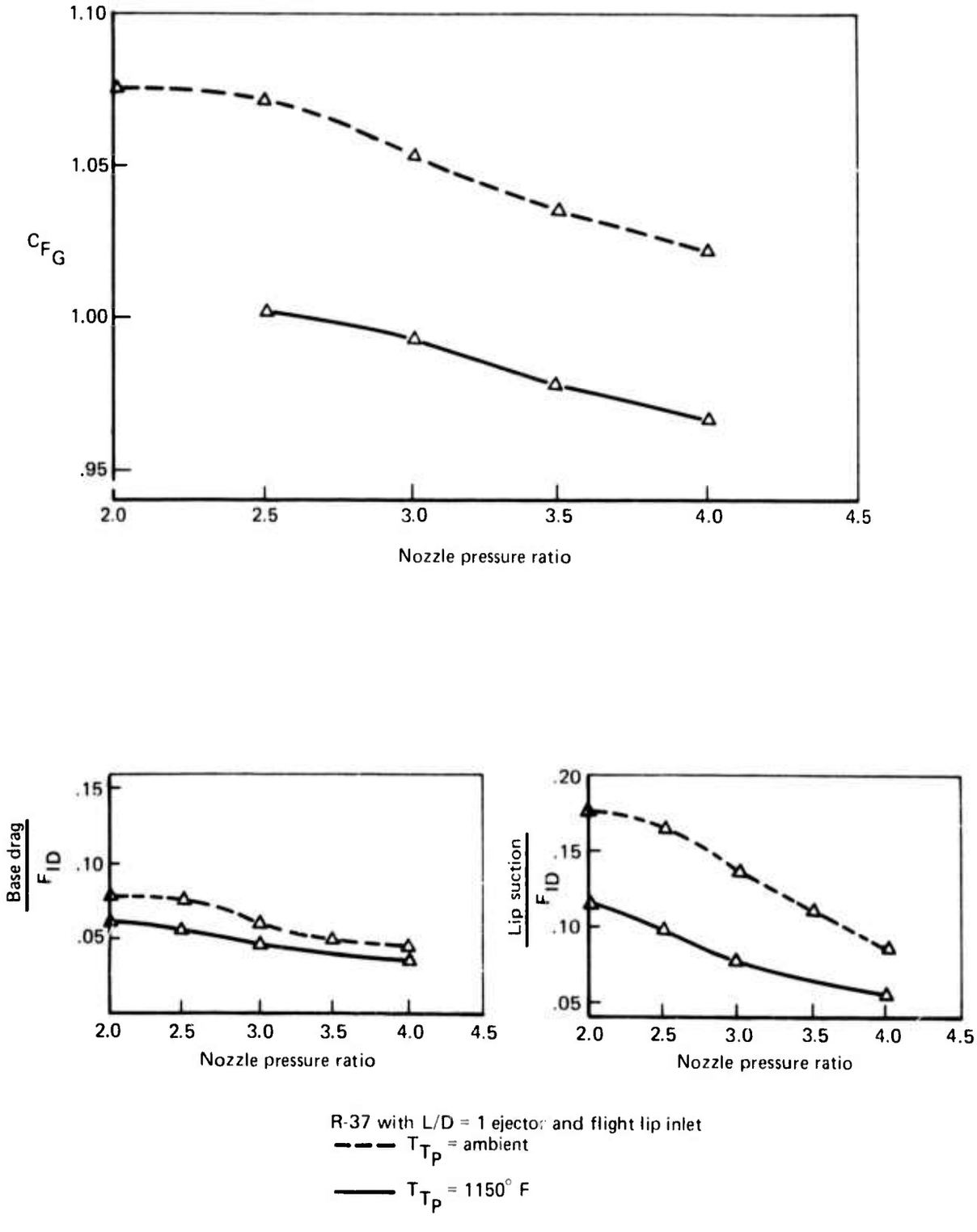

Figure 27.—Effect of Primary Jet Temperature on Ejector Performance

The reduced lip suction reflects a decrease in ejector secondary air handling, which in turn reduces thrust agumentation. This effect, which is much larger than the temperature effect on base drag, governs the variations of the gross thrust coefficient with temperature.

The gross thrust coefficient decreases in a similar manner for other configurations at 1150°F, such as a round convergent nozzle with L/D = 3 ejector and bellmouth lip. Cold and hot jet gross thrust coefficients are plotted in figure 28. As mentioned earlier, this configuration is representative of a partial mixing phenomenon. A maximum gross thrust coefficient is observed at a pressure ratio of about 2.5 when the primary flow is at ambient temperature; for the high temperature case, no such maximum is observed. This can be explained by the fact that the mixing process is enhanced at high temperature, because it is closer to fully mixed flow than in the cold flow case.

- Temperature effects on ejector air handling
  The addition of heat results in a decrease of the mass flow augmentation ratio in all cases. This can be predicted analytically for the round convergent nozzle by using a one-dimensional analysis that assumes full mixing. The predicted loss amounts to about 10% of the mass flow augmentation ratio, which corresponds closely to experimental results. The slope of the predicted ratios is related to the choice of a correct inlet loss $\Delta P_T/q$. The prediction is indicated in figure 22 with the experimental data curves for the R/C nozzle and L/D = 6 (fully mixed) ejector.

  The temperature effect is of the same magnitude for the fully mixed R/C configuration and for the multitube nozzle case, figure 23. For the round convergent nozzle with a short ejector the effect is similar as shown in figure 29.

3.5 EJECTOR FLOW MIXING

Ejector flow mixing was investigated through measurement of static pressures along the ejector walls, and total pressure and temperature traverses at various stations within the ejectors. Mixing profiles for the R/C nozzle with L/D = 3 and L/D = 6 ejectors are compared with a theoretical evaluation based on a partial mixing hypothesis (ref. 7 and 8).

3.5.1 EJECTOR WALL PRESSURES

Static pressure taps have been located every few inches along the ejector's walls (see fig. 9). The pressure variations can be followed, up to the exit of each ejector, for a series of pressure ratios (figs. 24 and 25). At a pressure ratio of 2.0 the secondary air entrained is at fairly low velocity (M = 0.35 for the L/D = 6 ejector with the bellmouth lip) at the inlet plane of the ejector, and the static pressure is increased smoothly to match ambient conditions at the exit. As the pressure ratio is increased, the primary flow becomes underexpanded at the primary nozzle exit and undergoes a series of expansions and contractions as it moves through the ejector. This is reflected in the secondary flow, which is accelerated during the primary flow expansion phases (low static pressure) and decelerated during the contraction phases. The phenomenon becomes more obvious as the pressure ratio is raised, but the secondary flow does not seem to reach choked conditions (M_S = 0.66 at PR = 4) for the L/D = 1 ejector with the bellmouth lip. With the shorter L/D = 3 ejector, the velocity of the secondary flow is lower than with the L/D = 6 ejector, and the underexpansion of the primary flow is not as noticeably reflected.

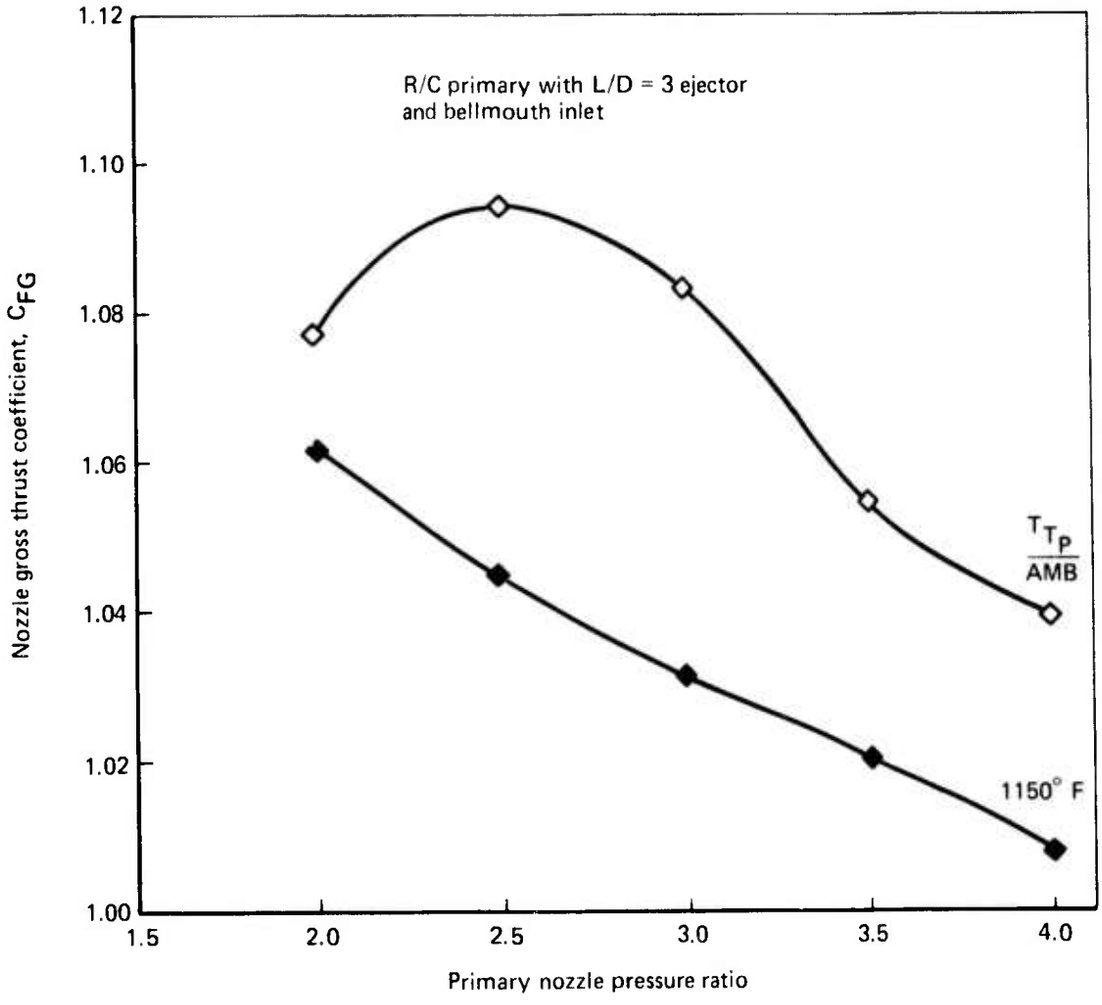

Figure 28.–Effect of Temperature on Performance–Partially Mixed Ejector Flow

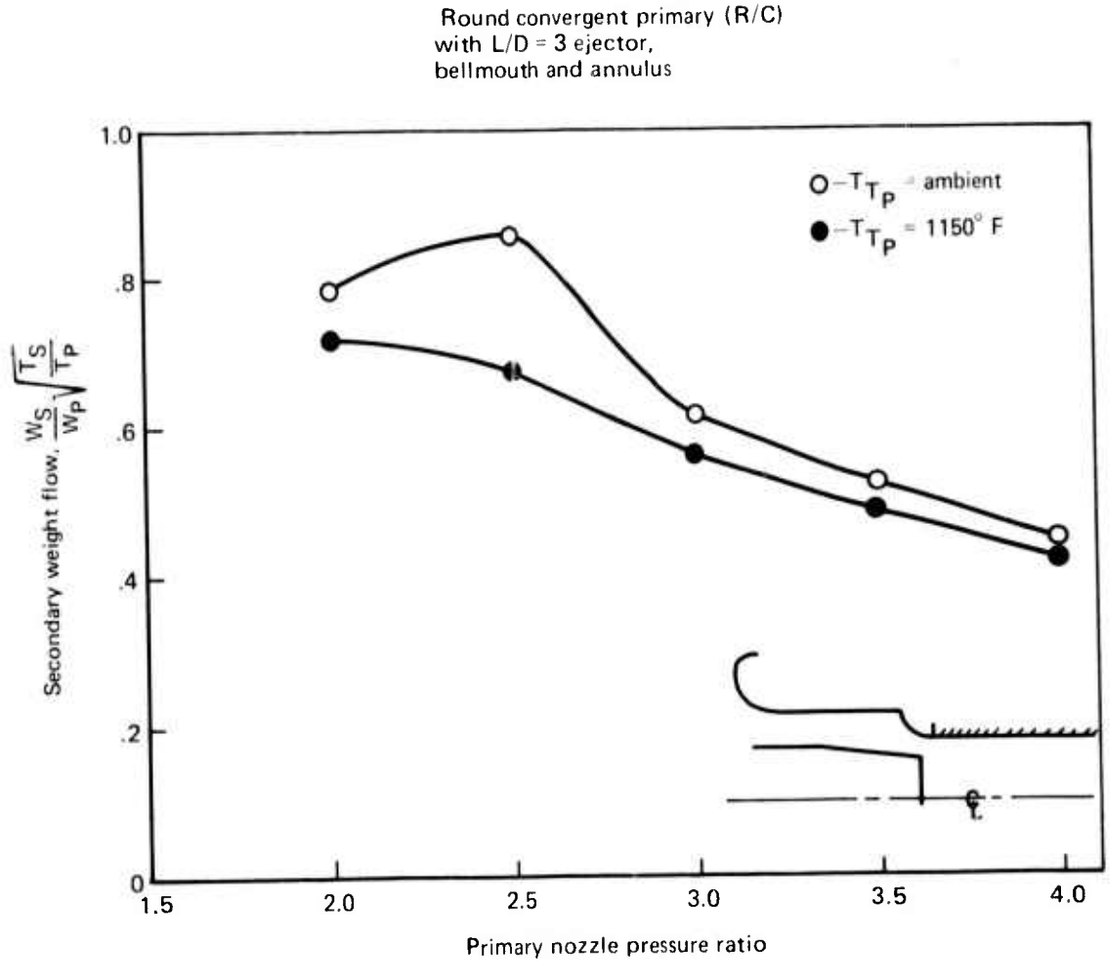

Figure 29.—Secondary Mass Flow for a Partially Mixed R/C Configuration

3.5.2 MIXING PROFILES

- Round convergent nozzle
  Total pressure and temperature traverses were taken at the primary nozzle exit plane within the ejector (at 8 in. and 24 in. downstream for the L/D = 6 ejector and 8 in. only for the ejector with L/D = 3) and at the ejector exit plane.

  In order to obtain information on the mixing rate within ejectors of different lengths and to correlate it with the variations in mass flow, total pressure and temperature plots were compared for the two configurations below at PR = 2.0 and T_{T_P} = 1150°F, and also at T_{T_P} = ambient.

  - Round-convergent nozzle, L/D = 6 ejector, bellmouth inlet with flow annulus
  - Round-convergent nozzle, L/D = 3 ejector, bellmouth inlet with flow annulus

  Plots of the total pressure and temperature traverses are shown in figures 30 through 33. Theoretical predictions for these profiles are also included.

  Nozzle exit plane profiles are similar for both configurations. Departure from the theoretically square total pressure profile seems indicative of a small boundary layer that would have built up inside the nozzle. The total temperature profile (for a total primary temperature of 1150°F) differs somewhat from predictions; this is probably because of the instrumentation. Nonsymmetrical profiles resulted when the shielded temperature probe would not cool off instantly after relatively rapid transition from hot flow to ambient.

  At a station 8 in. downstream from the primary nozzle, traverses taken inside both ejectors do not show any major differences, but at 24 in. downstream the total temperatures and pressures at the center of the core are indicative of different decay rates.

  At the exit of the L/D = 3 ejector (24 in. downstream of primary nozzle) approximately one-tenth of the flow still retained the original total pressure of the primary flow P_{T_P} = 26 psi and T_{T_P} = 940°F. This difference in mixing rate within the ejectors is related to the difference in secondary flow rate for both configurations.

  If the ejectors' exit profiles are compared, it becomes obvious that the mixing process is at a much more advanced stage at the exit of the L/D = 6 ejector than at the exit of the L/D = 3 ejector. The traverses indicate that the flow is relatively well mixed at the L/D = 6 ejector exit although not fully mixed (the variations between the centerline total pressure and total pressures near the wall are still of the order of 7_{psi}, the corresponding temperature difference approaches 700°R).

- 37-tube nozzle
  Traverses have been taken for the R/37 multitube suppressor nozzle with the short L/D = 1 ejector and the large bellmouth configuration. These indicate the state of mixing at the exit of the ejector for PR = 2 and PR = 4, the total temperature being ambient. At PR = 2, the mixing rate seems to be comparable to that observed for the R/C, with

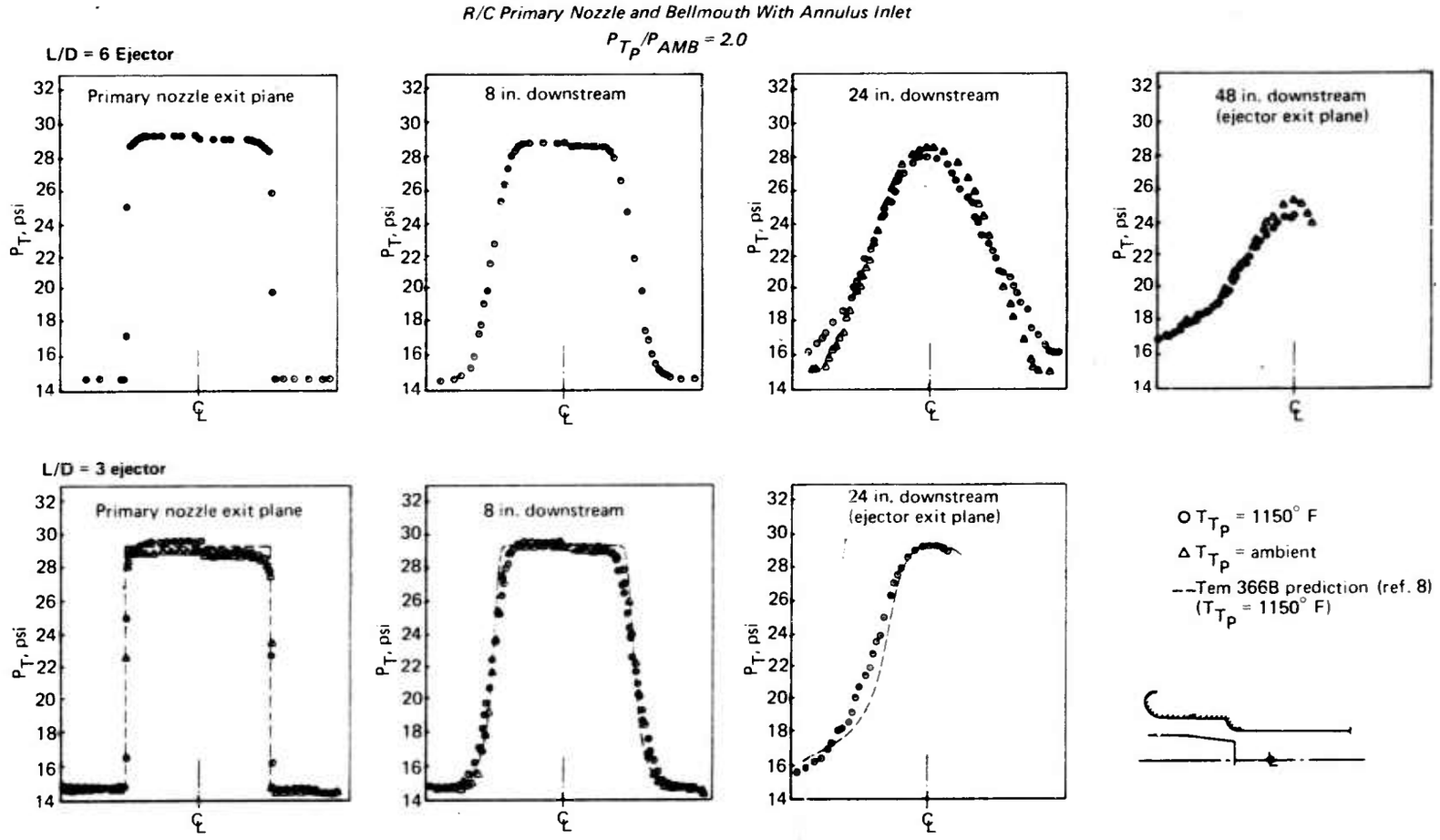

Figure 30.—Downstream Total Pressure Profiles for R/C Configurations

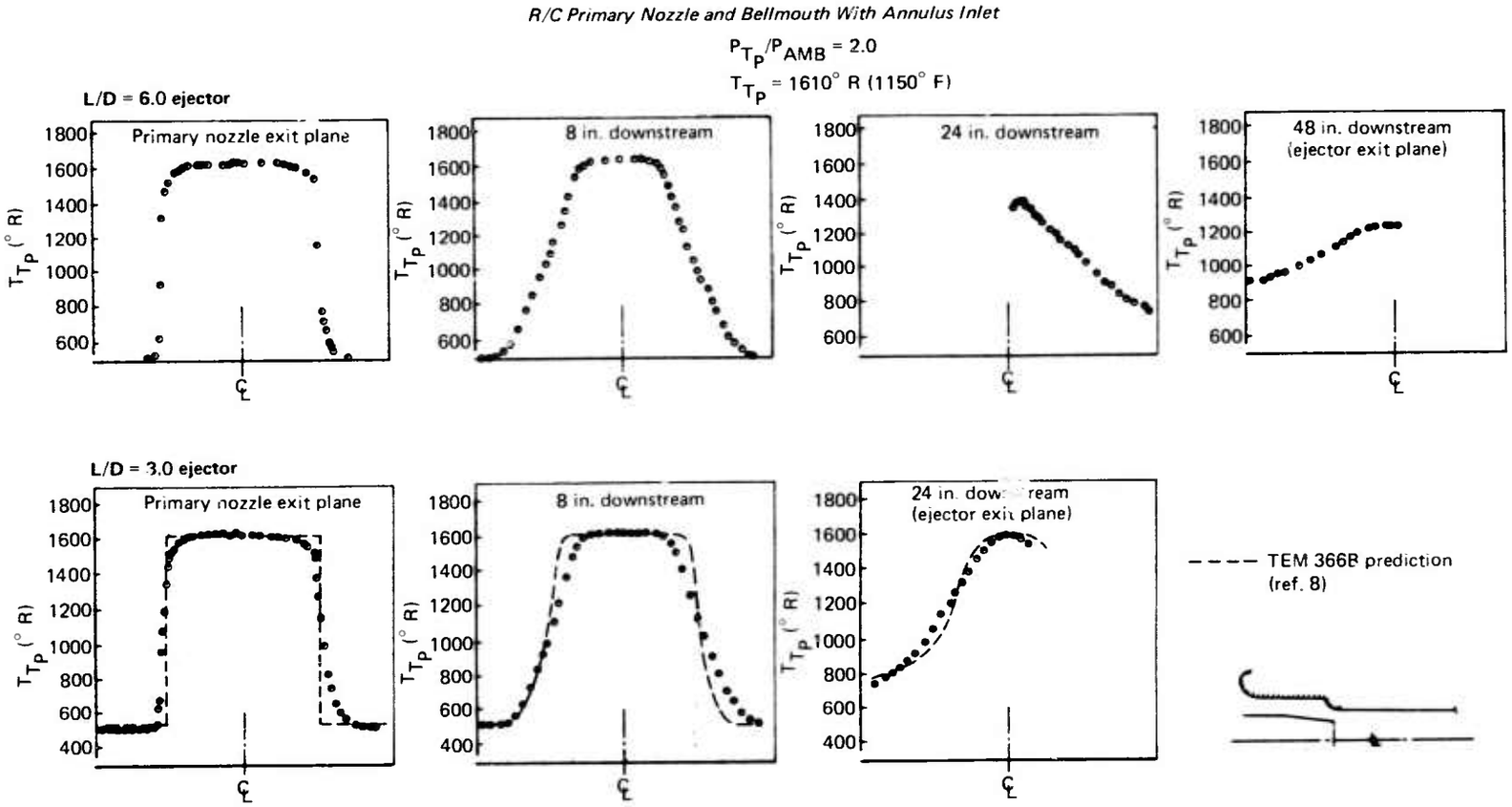

Figure 31.—Downstream Total Temperature Profiles for R/C Configurations

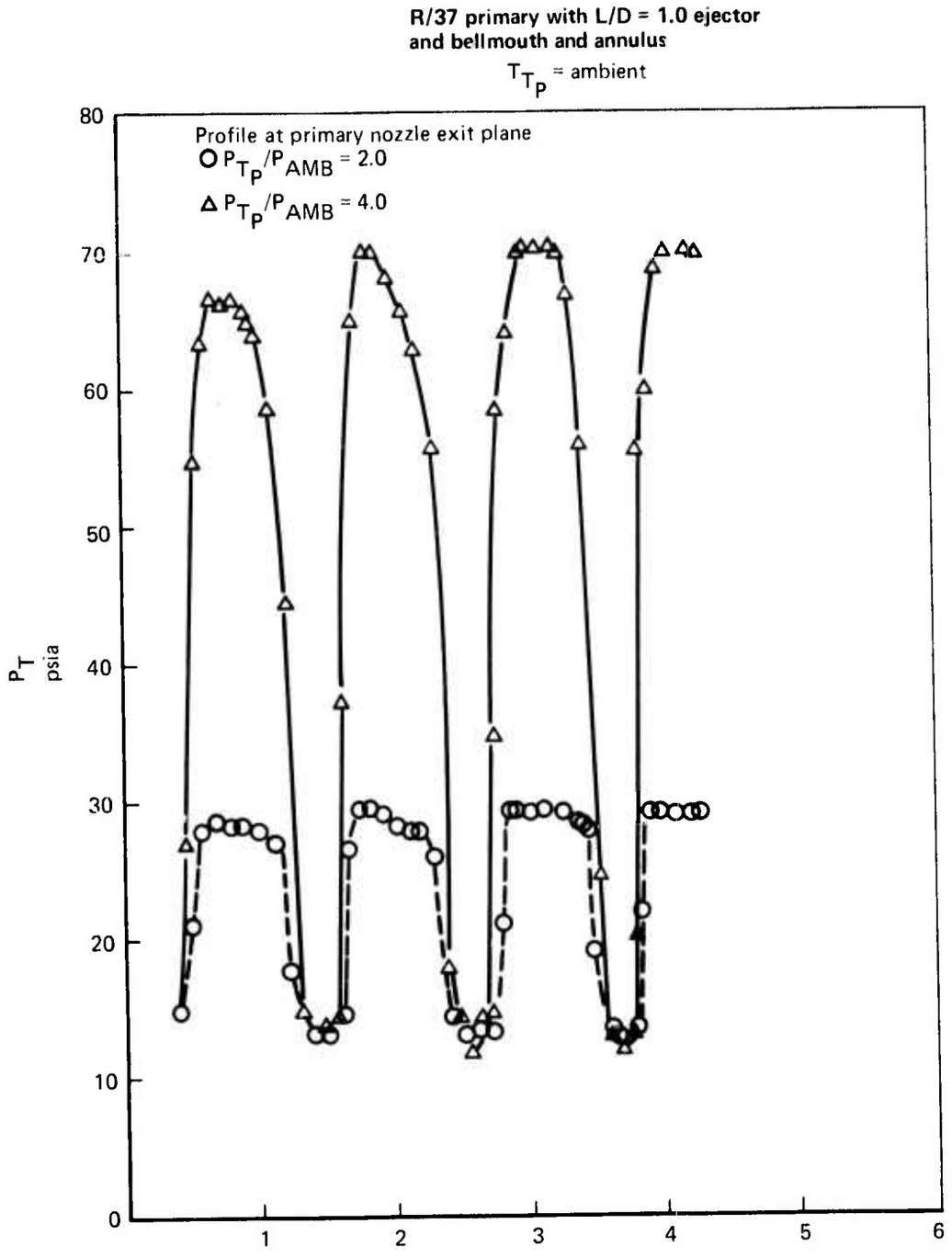

Figure 32.—Total Pressure Profile at Suppressor Nozzle Exit Plane

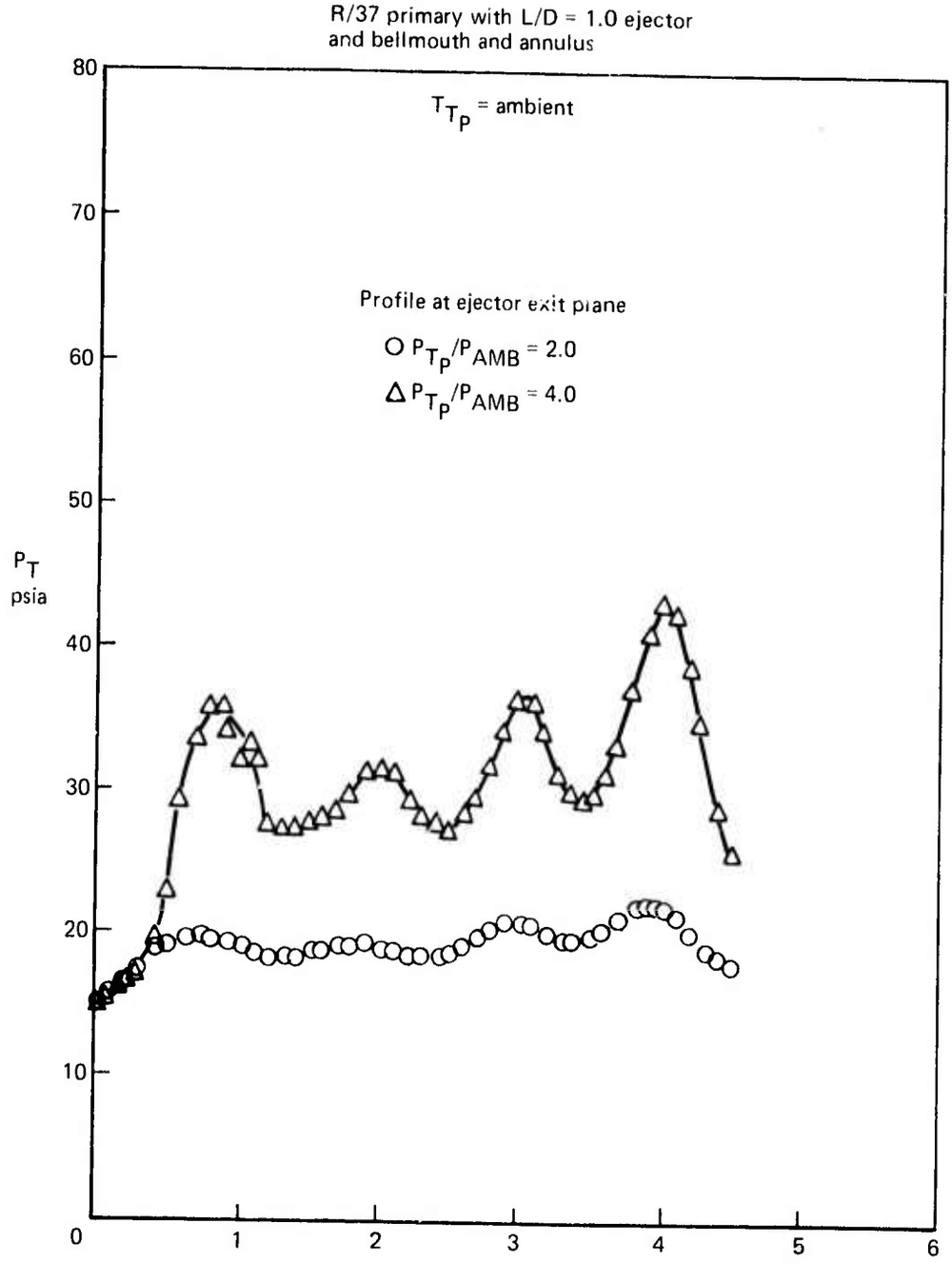

Figure 33.—Total Pressure Profile at Ejector Exit Plane

L/D = 6 ejector configuration. At PR = 4 it is not certain that the flow is fully mixed. The profiles plotted in figures 32 and 33 also show that the mixing varied with the location of the individual jets and that the flow was not evenly distributed at the nozzle exit (the outer row of tubes having a lower pressure) because of losses in the longer tubes. It can be seen, for example, that at high pressure ratios, the jets from the inner tubes were mixing faster with the surrounding media than the jets coming from the outer row of tubes. (Inspection of the individual base static taps indicates that the base is well ventilated, allowing for good mixing of the flow originating from the second row of tubes.)

REFERENCES

1. C. Wright, D. Morden, and C. Simcox, *SST Technology Follow-On Program—Phase I; A Summary of the SST Noise Suppression Test Program,* AD-900-401L, Federal Aviation Administration, Washington, D.C., February 1972.

2. J. Atvars, et al., *Development of Acoustically Lined Ejector Technology for Multitube Jet Noise Suppressor Nozzles by Model and Engine Tests Over a Wide Range of Jet Pressure Ratios and Temperatures,* D6-60226.

3. J. Cclehour, *A Potential Flow-Boundary Layer Iteration Method to Predict Drag for Two-Dimensional and Axi-Symmetric Bodies,* D6-22777, December 1970.

4. "Test Data Report—Parametric Test of Conical Convergent Nozzles," (Unpublished report).

5. J. E. Postlewaite, "Thrust Performance of Suppressor Nozzles," *Journal of Aircraft,* vol. 3, November 1966.

6. Anon., "Aerodynamic Design—Air Intake," *Aircraft Engineering,* Hawker Siddeley, December 1969.

7. T. A. Reyhner, *Calculation of Internal Flow Fields of Two-Dimensional and Axisymmetric Ejectors (TEM 366),* D6-40936, November 1973.

8. T. A. Reyhner, *Comparison of TEM 366B Predictions with Measured Flow in an Ejector Operating at a Pressure Ratio of 2.0,* ME-RES-1683, October 1973.